Optimal Binary Signaling for Correlated Sources over the Orthogonal Gaussian Multiple-Access Channel

by

Tyson Mitchell

A report submitted to the
Department of Mathematics and Statistics
in conformity with the requirements for
the degree of Master of Science

Queen's University
Kingston, Ontario, Canada
November 2014

Abstract

Optimal binary communication, in the sense of minimizing symbol error rate, with nonequal probabilities has been derived in [1] under various signalling configurations for the single-user case with a given average energy E. This work extends a subset of the results in [1] to a two-user orthogonal multiple access Gaussian channel (OMAGC) transmitting a pair of correlated sources, where the modulators use a single phase or basis function and have given average energies E_1 and E_2, respectively. These binary modulation schemes fall in one of two categories: (1) transmission signals are both nonnegative, or (2) one transmission signal is positive and the other negative. To optimize the energy allocations for the transmitters in the two-user OMAGC, the maximum a posteriori detection rule, probability of error, and union error bound are derived. The optimal energy allocations are determined numerically and analytically. Both results show that the optimal energy allocations coincide with corresponding results from [1]. It is demonstrated in Chapter 3 that three parameters are needed to describe the source. The optimized OMAGC is compared to three other schemes with varying knowledge about the source statistics, which influence the optimal energy allocation. A gain of at least 0.73 dB is achieved when $E_1 = E_2$ or $2E_1 = E_2$. When $E_1 \gg E_2$ a gain of at least 7 dB is observed.

Acknowledgments

First and Foremost, I would like to thank my supervisors, Dr. Fady Alajaji and Dr. Tamás Linder for their patience, guidance, and support. I thank Dr. Tamás Linder for approaching me at the end of my undergraduate degree with the opportunity of studying under his guidance. Further, I thank Dr. Fady Alajaji for the topic of this report.

I am also grateful to my parents, for their unwavering love and support in all my academic endeavours. I am also thankful to my brother for always sharing a joke or two.

Lastly, I would like to thank my beloved Hayley, for keeping me grounded throughout my graduate-level studies.

Contents

List of Tables

List of Figures

Chapter 1

Introduction

1.1 Digital Communication Systems

Digital communication systems are comprised of a number of elements, each with a counterpart. Figure 1.1 illustrates a functional diagram and the elements of a typical communication system.

All digital communication systems begin with a source. The source can be an analog signal, such as audio or video, or a digital signal, such as computer data. The source produces messages that must be converted into sequences of elements from a finite alphabet, usually binary. Representing the output of an analog or digital source as a sequence of elements from a finite alphabet is known as source coding, where, ideally, the output of the source is represented using as few elements as possible [2]. Source coding provides methods of eliminating redundancy from the source. The output of the source coder, known as the information sequence, is then passed to the channel coder. The purpose of the channel coder is to add redundancy, in a controlled manner, into the information sequence, which can be used after transmission to overcome the effects of noise and interference due to the channel [2]. This process aims to increase the reliability of the received information sequence. The output sequence from the channel coder arrives at the modulator,

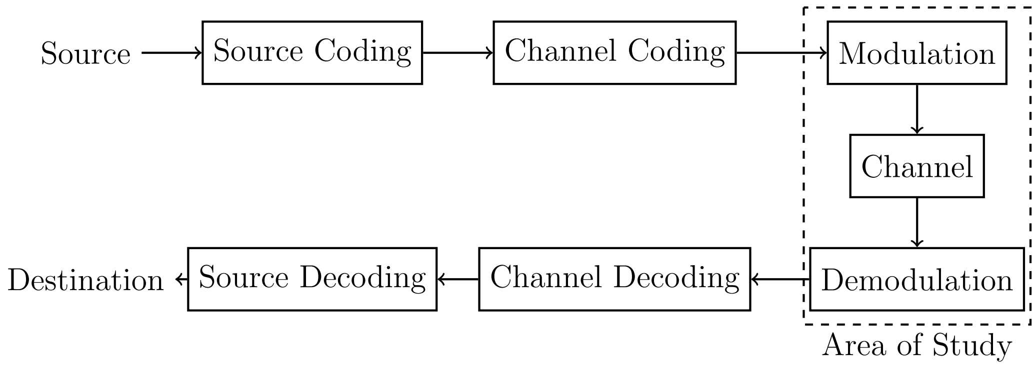

Figure 1.1: Block diagram representing the components of a communication system, with a highlighted area of the topic relevant to this document.

which servers as an interface to the communications channel [2]. The main purpose of the modulator is to map the channel-coded information sequences into signal waveforms.

After transmission, information is received at the demodulator. The demodulator receives and processes the channel-corrupted waveforms and reduces them to symbols representing an estimate of the modulated data sequence [2]. This estimate is passed to the channel decoder, which using the added redundancy introduced in the channel encoder, attempts to reconstruct the original information sequence from knowledge of the code used by the channel coder and the redundancy contained in the received data. Lastly, the source in reconstructed via the source decoder at the destination. If an analog output is desired, the source decoder accepts the output sequence from the channel decoder and attempts to reconstruct the original signal from the source, using knowledge of the source coding method [2]. However, from errors that may have occurred during reconstruction, the source may be corrupted or distorted.

It should be noted that the demodulation just described is often referred to as hard-decision detection. Demodulation and channel decoding may be combined in one step; this is a topic of soft-decision detection and is not considered in this work.

1.2 Motivation

This report focuses on modulation and demodulation. The goal is to determine the optimal energy allocations of two binary modulation schemes that transmit to a common receiver, such that the data sequences entering the transmitters are positively correlated. A detailed description of the problem and system is given in Chapter 3. At the core, this report extends a subset of the results in [1] by Korn *et al.* from a single-user additive white Gaussian noise channel to a two-user orthogonal multiple access Gaussian channel (OMAGC). As it is intuitively unclear where the optimal energies will lay, it will be interesting to see if the optimal energies of the OMAGC coincide with results from [1].

1.3 Contributions

To our knowledge, this problem has not been investigated. To find if the optimal communication schemes for single-user and two-user systems coincide, a number of important results must be derived. For the two-user case, these results are: a probability of symbol error calculation, along with a corresponding upper bound. The single-user results are found in [1]. Next, the optimal transmission energies are numerically determined using the error probability and analytically determined using the upper bound. From these results, it is shown that the optimal transmission energies coincide with the single-user case.

1.4 Organization of Report

Chapter 2 reviews maximum a posteriori detection from the perspective of a typical digital communication text, followed by a summary of the relevant results of [1]. The system model, description of the source and the maximum a posteriori detection rule are given in Chapter 3, where also, the system error probability and union error bound are derived. Chapter 4 contains a verification of the probability of error calculations, numerical optimization, analytical optimization, and performance comparisons. Chapter 5 presents conclusions and discussions of future work.

Chapter 2

Background

2.1 MAP Detection for Single-User Systems

When discussing modulation and demodulation for single-user communication systems, it is convenient to introduce constellations points. Modulators consist of a set of basis functions $\{\psi_1, \psi_2, \dots, \psi_N\}$, where each $\psi_i : [0, T] \mapsto \mathbb{R}$ and has unit energy, i.e. $\int_0^T \psi_i^2(t)dt = 1$ for $i = 1, \dots, N$, where $T > 0$ is finite and $\mathbb{R}$ denotes the real numbers. Outputs from the channel coder will be mapped to linear combinations of the basis functions. Note, if the channel coder output sequences of length k, the modulator may look at sequences of length l at a time. Supposing there are M constellation points, each signal $\boldsymbol{s}_m$ can be written as

$$\boldsymbol{s}_m(t) = a_{1m}\psi_1(t) + a_{2m}\psi_2(t) + \cdots + a_{Nm}\psi_N(t)$$

where $m \in \{1, \dots, M\}$ and $a_{ij} \in \mathbb{R}$ for $i \in \{1, \dots, N\}$ and $j \in \{1, \dots, M\}$. Thus, $\mathcal{S} = \{\boldsymbol{s}_m | m = 1, \dots, M\}$ is the set of transmission signals or constellation points. Further define $\boldsymbol{n}(t) = (n_1(t), \dots, n_N(t))$ to be an N-tuple from an additive white Gaussian noise (AWGN) process, where the $n_i(t)$ are independent Gaussian random variables with zero mean and variance σ^2 for $i = 1, \dots, N$. Define $\boldsymbol{r} = \boldsymbol{s} + \boldsymbol{n}$ to be the observation vector of the received values, where $\boldsymbol{s} \in \mathcal{S}$, and addition is completed component wise.

For optimal signal detection the goal is to maximize the probability that the received vector $\boldsymbol{r}$ is correctly mapped back to the transmitted signal $\boldsymbol{s}$. As a result, a decision rule based on the posterior probabilities is defined as

$$P(\text{signal } \boldsymbol{s} \text{ is transmitted}|\boldsymbol{r})$$

shortened to $P(\boldsymbol{s}|\boldsymbol{r})$ [2]. In this case the detected constellation point $\hat{\boldsymbol{s}}$ is given as

$$\hat{\boldsymbol{s}} = \arg\max_{\boldsymbol{s}\in\mathcal{S}} P(\boldsymbol{s}|\boldsymbol{r}). \tag{2.1}$$

In words, the decision criterion requires selecting the signal corresponding to the maximum of the set of posterior probabilities $\{P(\boldsymbol{s}_m)|\boldsymbol{r})\}_{m=1}^{M}$ [2]. It is shown in [2], that this criterion maximizes the probability of correct decision and, thus, minimizes the probability of error. This decision rule is called maximum a posterior (MAP) detection. Now, using Bayes' Rule, the above can be written as

$$\hat{\boldsymbol{s}} = \arg\max_{\boldsymbol{s}\in\mathcal{S}} \frac{f(\boldsymbol{r}|\boldsymbol{s})P(\boldsymbol{s})}{f(\boldsymbol{r})}$$

where $f(\boldsymbol{r}|\boldsymbol{s})$ is the conditional probability density function (PDF) of the observation vector $\boldsymbol{r}$ given that $\boldsymbol{s} \in \mathcal{S}$ was sent and $P(\boldsymbol{s})$ is the a priori probability that $\boldsymbol{s} \in \mathcal{S}$ was sent. Further, since the denominator of the above is not dependent on $\boldsymbol{s}$, the expression becomes

$$\hat{\boldsymbol{s}} = \arg\max_{\boldsymbol{s}\in\mathcal{S}} f(\boldsymbol{r}|\boldsymbol{s})P(\boldsymbol{s}).$$

From here, most communication texts note that simplifications occur when $P(\boldsymbol{s}) =$

$1/M$, i.e., all constellation points are equiprobable. In this case, the decision rule becomes

$$\hat{\boldsymbol{s}} = \arg\max_{\boldsymbol{s} \in \mathcal{S}} f(\boldsymbol{r}|\boldsymbol{s})$$

which is the so-called maximum likelihood (ML) detection rule (see [2]). However, the simplification $P(\boldsymbol{s}) = 1/M$ is often unrealistic since it is known that speech, image and video data exhibit a bias to a subset of the transmission signal set (e.g. see [3], [4]).

2.2 Optimized Binary Signalling Over Single-User AWGN Channels

In [1], binary modulation schemes are considered for the point-to-point AWGN channel. Consequently, only two constellation points s_1 and s_2, based on two (unit-energy) basis functions ψ_1 and ψ_2 are needed. Thus, let

$$s_1(t) = \sqrt{E_1}\psi_1(t) \text{ and } s_2(t) = \sqrt{E_2}\psi_2(t)$$

be arbitrary binary signals given as functions of time, $t \in [0, T]$ for some positive, finite T, with energies given by

$$\int_0^T [\sqrt{E_i}\psi_i(t)]^2 dt = E_i$$

for $i = 1, 2$ having probabilities $0 \leq p_1 = p \leq 0.5$, $p_2 = 1 - p$, respectively. Let γ be the correlation between $\psi_1(t)$ and $\psi_2(t)$, given by

$$\gamma = \int_0^T \psi_1(t)\psi_2(t)dt, \ -1 \leq \gamma \leq 1$$

where we are interested in the cases when $\psi_1(t) = \psi_2(t)$ and $-\psi_1(t) = \psi_2(t)$ which result in $\gamma = 1$ and $\gamma = -1$, respectively. We call these modulation systems single-phase modulation schemes. The average energy per bit (or signal) is given by

$$E = pE_1 + (1-p)E_2. \tag{2.2}$$

After sending $s(t) \in \{s_1(t), s_2(t)\}$ over the channel, the received signal is given by

$$r(t) = s(t) + n(t)$$

where $n(t)$ is an AWGN process with power spectral density (PSD) $\sigma^2 = N_0/2$. The goal of [1] is to derive the optimal energies E_1 and E_2 which minimize the bit error probability (BEP) given E, where the BEP is given by

$$P(e) = P(s_2(t)|s_1(t))p + P(s_1(t)|s_2(t))(1-p) \tag{2.3}$$

where $P(s_i(t)|s_j(t)) = P(\hat{\boldsymbol{s}} = s_i(t)|\boldsymbol{s} = s_j(t))$ is the probability that MAP detection selects $s_i(t)$ given that $s_j(t)$ was transmitted over the channel for $i, j \in \{1, 2\}$ and $i \neq j$. It is shown in [1], using [5], that the above BEP can be written as

$$P(e) = Q\left(\sqrt{A} - \frac{B}{\sqrt{A}}\right)p + Q\left(\sqrt{A} + \frac{B}{\sqrt{A}}\right)(1-p)$$

where

$$A = \frac{E_1 + E_2 - 2\gamma\sqrt{E_1 E_2}}{2N_0},$$
$$B = (1/2)\ln(p/(1-p)),$$

and

$$Q(x) = \frac{1}{\sqrt{2\pi}} \int_x^\infty \exp\left(-\frac{u^2}{2}\right) du.$$

It is proved in [1], that $P(e)$ is a decreasing function of A, implying that $P(e)$ is minimized when A is maximized. Next we note that

$$A = \frac{E_1 + \frac{E - E_1 p}{1-p} - 2\gamma\sqrt{\frac{E_1 E - E_1^2 p}{1-p}}}{2N_0}$$

since

$$E_2 = \frac{E - E_1 p}{1 - p}. \tag{2.4}$$

The problem becomes finding the optimal value of $E_1 \in [0, E/p]$. The relevant case to this report is when $\gamma \neq 0$, i.e., the case of nonorthogonal signalling. Consider the first and second derivatives of A with respect to E_1:

$$\begin{aligned}
\frac{\partial A}{\partial E_1} &= \frac{1}{2N_0}\left[\frac{1-2p}{1-p} - \frac{\gamma E(E - 2E_1 p)}{\sqrt{1-p}(EE_1 - E_1^2 p)}\right], \\
\frac{\partial^2 A}{\partial E_1^2} &= \gamma \frac{2p(EE_1 - E_1^2) + (E - 2E_1 p)^2}{2\sqrt{(1-p)}(EE_1 - E_1^2 p)^{3/2} N_0}.
\end{aligned}$$

Thus, the location of the maximum is dependent on γ.

Case 1: $\gamma > 0$: In this case, it is shown in [1] that A is convex with respect to E_1. So the maximum occurs at a boundary point. Since $E_1 \in [0, E/p]$, [1] shows that $E_1 = E/p$ and $E_2 = 0$ are the optimal energies; this is the on-off keying (OOK) signalling scheme.

Case 2: $\gamma < 0$: In this case, it is shown in [1] that A is a concave function of E_1 and attains a maximum when $E_1 \in (0, E/p)$. The optimal E_1 in this case is given by

$$E_1 = \frac{E}{2p}\left[1 + \frac{1-2p}{\sqrt{1 - 4p(1-p)(1-\gamma^2)}}\right].$$

The above result is obtained after setting $\partial A / \partial E_1 = 0$. From (2.2), the optimal E_2 is then given by

$$E_2 = \frac{E}{2(1-p)} \left[1 - \frac{1-2p}{\sqrt{1-4p(1-p)(1-\gamma^2)}} \right].$$

As previously mentioned, the case of interest is nonorthogonal signalling, in particular when $\gamma = 1$ and $\gamma = -1$. For $\gamma = 1$, the optimal energies (from Case 1 above) are

$$E_1 = E/p \text{ and } E_2 = 0, \tag{2.5}$$

which is OOK, and for $\gamma = -1$, which corresponds to binary pulse-amplitude modulation (BPAM), the optimal energies are given (from Case 2 above) as

$$E_1 = \frac{E}{2p} \left[1 + \frac{1-2p}{\sqrt{1-4p(1-p)(1-\gamma^2)}} \right] = \frac{E(1-p)}{p}, \tag{2.6}$$

$$E_2 = \frac{E}{2(1-p)} \left[1 - \frac{1-2p}{\sqrt{1-4p(1-p)(1-\gamma^2)}} \right] = \frac{Ep}{1-p}. \tag{2.7}$$

Chapter 3

MAP Detection and Probability of Error

3.1 Problem Definition

As outlined in the previous chapter, the optimal energy allocation for binary communication with nonequal probabilities over a single-user AWGN channel has been determined [1]. This report extends the results of [1] to a two-user orthogonal multiple access Gaussian Channel (OMAGC) with a correlated source.

First we define our problem and introduce our assumptions and notations. Let, $\{(U_1^{(n)}, U_2^{(n)})\}$ be pairs of an independent and identically distributed (i.i.d.) sequence of binary-valued random variables, such that $U_i^{(n)} \in \{0, 1\}$ and $0 \leq P(U_i^{(n)} = 0) = p_i < 0.5$ for $n = 1, 2, 3, \ldots$ and $i = 1, 2$. Further, for $n = 1, 2, 3, \ldots$ let ρ be the correlation coefficient between $U_1^{(n)}$ and $U_2^{(n)}$. Also, we assume for all n, $(U_1^{(n)}, U_2^{(n)})$ follows the joint probability mass function $p_{U_1,U_2}(u_1, u_2)$ defined in Section 3.3.

The basis functions represent the physical frequencies, or modulated phases, used by a transmitter. Transmitter 1 will use $\{\psi_1^{(1)}, \psi_2^{(1)}\}$ as basis functions and Transmitter 2 will use $\{\psi_1^{(2)}, \psi_2^{(2)}\}$ as basis functions, such that Transmitters 1 and 2 have correlation γ_1 and γ_2, respectively. Thus, we are interested in the cases when $\gamma_1 = \gamma_2 = -1, 1$ and $\gamma_1 = -\gamma_2$. When $\gamma_1 = \gamma_2 = 1$ the transmitters may only implement positive-valued signals (as $\psi_1^{(i)} = \psi_2^{(i)}$ for $i = 1, 2$). Whereas, when

$\gamma_1 = \gamma_2 = -1$ the transmitters will use one positive-valued signal and one negative-valued signal (as $-\psi_1^{(i)} = \psi_2^{(i)}$ for $i = 1, 2$). When $\gamma_1 = -\gamma_2$, without loss of generality we assume $\gamma_1 = 1$. Recall that these modulation systems are referred to as single-phase modulation schemes. At time instance n, $U_1^{(n)}$ and $U_2^{(n)}$ are modulated independently of one another to carrier signals $s_1^{(n)}$ and $s_2^{(n)}$, respectively, across two independent AWGN memoryless channels having Gaussian noise processes $\{N_1^{(n)}\}$ and $\{N_2^{(n)}\}$, where $N_1^{(n)}$ and $N_2^{(n)}$ have zero mean and variance σ_1^2 and σ_2^2, respectively, for all n. For joint MAP detection at time instance n, the received pair is given by $(R_1^{(n)}, R_2^{(n)})$, where $R_i^{(n)} = s_i^{(n)} + N_i^{(n)}$ for $i = 1, 2$. The system model is depicted in Figure 3.1.

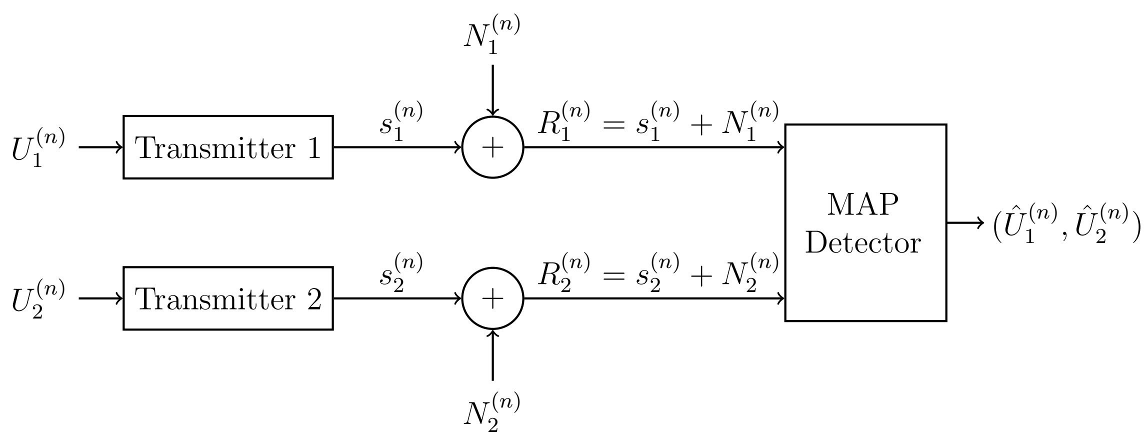

Figure 3.1: Block diagram of the system model.

In this report we use uppercase letters to denote random variables and lowercase letters to represent the corresponding realizations. The goal of this report is to determine the optimal energies, which minimize the joint symbol error rate (SER) under joint MAP detection, for each constellation point used by Transmitters 1 and 2, which do not communicate with one another. We do not necessarily assume that the transmitters implement identical constellation maps. Lastly, we assume coherent detection and bandpass modulation and demodulation with no restrictions on bandwidth.

3.2 Modulation

The modulation schemes when $\gamma_1 = \gamma_2 = 1$, $\gamma_1 = \gamma_2 = -1$, and $-\gamma_2 = \gamma_1 = 1$ are illustrated in Figures 3.2, 3.3, and 3.4, respectively, where Transmitters 1 and 2 have constellation points $s_{10} = \sqrt{E_{10}}\gamma_1$, $s_{11} = \sqrt{E_{11}}$ and $s_{20} = \sqrt{E_{20}}\gamma_2$, $s_{21} = \sqrt{E_{21}}$, respectively. Let $\mathcal{S}_1 = \{s_{10}, s_{11}\}$, and $\mathcal{S}_2 = \{s_{20}, s_{21}\}$ be the set of transmission signals for Transmitters 1 and 2, respectively.

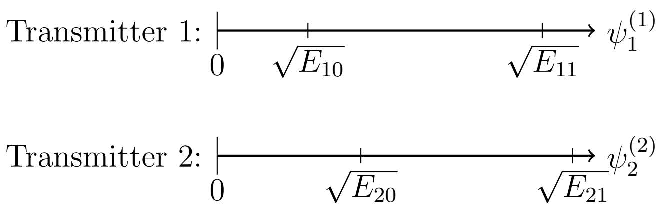

Figure 3.2: Modulation scheme for Transmitter 1 and 2 when $\gamma_1 = \gamma_2 = 1$.

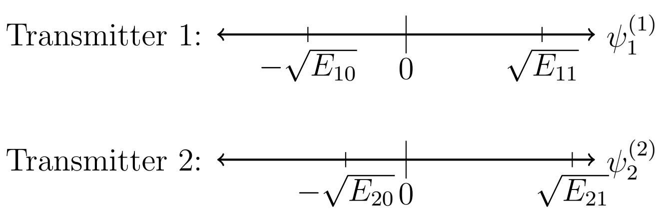

Figure 3.3: Modulation scheme for Transmitter 1 and 2 when $\gamma_1 = \gamma_2 = -1$.

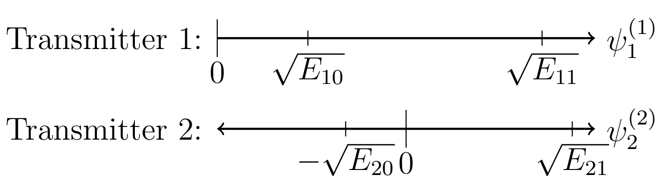

Figure 3.4: Modulation scheme for Transmitter 1 and 2 when $\gamma_1 = -\gamma_2 = 1$.

3.3 Full Description of the Source

We need only three terms to describe the i.i.d. binary correlated source $\{(U_1^{(n)}, U_2^{(n)}\}$. First, by definition

$$\rho = \mathrm{Cor}(U_1^{(n)}, U_2^{(n)}) = \frac{\mathrm{Cov}(U_1^{(n)} U_2^{(n)})}{\sqrt{\mathrm{Var}(U_1^{(n)})\mathrm{Var}(U_2^{(n)})}}$$

where $\mathrm{Cor}(U_1^{(n)}, U_2^{(n)})$ is the correlation coefficient between $U_1^{(n)}$ and $U_2^{(n)}$, $\mathrm{Cov}(U_1^{(n)}, U_2^{(n)})$ is the covariance of $U_1^{(n)}$ and $U_2^{(n)}$, and $\mathrm{Var}(U_i^{(n)})$ is the variance of $U_i^{(n)}$ for $i = 1, 2$ and all n. Letting $p_{11} = P(U_1 = 1, U_2 = 1)$ and recalling $1 - p_1 = P(U_1 = 1)$, and $1 - p_2 = P(U_2 = 1)$, we have

$$\begin{aligned}
\mathrm{Cov}(U_1^{(n)}, U_2^{(n)}) &= E[U_1^{(n)} U_2^{(n)}] - E[U_1^{(n)}]E[U_2^{(n)}] \\
&= P(U_1^{(n)} = 1, U_2^{(n)} = 1) - P(U_1^{(n)} = 1)P(U_2^{(n)} = 1) \\
&= p_{11} - (1 - p_1)(1 - p_2)
\end{aligned}$$

and

$$\begin{aligned}
\mathrm{Var}(U_1^{(n)}) &= E[(U_1^{(n)})^2] - E[U_1^{(n)}]^2 \\
&= P(U_1^{(n)} = 1) - P(U_1^{(n)} = 1)^2 \\
&= p_1(1 - p_1).
\end{aligned}$$

Similarly,

$$\mathrm{Var}(U_2^{(n)}) = p_2(1 - p_2).$$

Thus,

$$\rho = \frac{p_{11} - (1 - p_1)(1 - p_2)}{\sqrt{p_1(1 - p_1)p_2(1 - p_2)}}$$

and

$$p_{11} = \rho\sqrt{p_1(1-p_1)p_2(1-p_2)} + (1-p_1)(1-p_2).$$

Thus, the joint probability mass function (PMF) of the two-dimensional binary source $\{(U_1^{(n)}, U_2^{(n)}\}$ is given by

$$p_{U_1,U_2}(u_1,u_2) = \begin{cases} 1-(1-p_1)-(1-p_2)+p_{11}, & \text{if } u_1 = u_2 = 0, \\ (1-p_1)-p_{11}, & \text{if } u_1 = 1, u_2 = 0, \\ (1-p_2)-p_{11}, & \text{if } u_1 = 0, u_2 = 1, \\ p_{11}, & \text{if } u_1 = u_2 = 1. \end{cases}$$

Thus, we need only p_1, p_2 and one of ρ or p_{11} to fully describe our source.

3.4 MAP Detection

By assumption our system is memoryless, so to ease the notation the time indexing will be dropped. To find the MAP decision rule we consider (2.1), written out for our system:

$$(\hat{s}_1, \hat{s}_2) = \underset{(s_1,s_2)\in\mathcal{S}_1\times\mathcal{S}_2}{\arg\max}\, P(S_1 = s_1, S_2 = s_2 | r_1, r_2)$$

where $s_i \in \mathcal{S}_i$ is a modulated constellation point for $i = 1, 2$. The above can be written more compactly as

$$\hat{\boldsymbol{s}} = \underset{\boldsymbol{s}\in\mathcal{S}_1\times\mathcal{S}_2}{\arg\max}\, P(\boldsymbol{s}|\boldsymbol{r}) \tag{3.1}$$

where $\hat{\boldsymbol{s}} \in \mathcal{S}_1 \times \mathcal{S}_2$ is the detected constellation point pair and $\boldsymbol{r} = (r_1, r_2)$ is the pair of received values from the channel. Using Bayes' rule

$$\hat{\boldsymbol{s}} = \underset{\boldsymbol{s}\in\mathcal{S}_1\times\mathcal{S}_2}{\arg\max}\, \frac{f_{R_1,R_2|S_1,S_2}(\boldsymbol{r}|\boldsymbol{s})P((S_1,S_2) = \boldsymbol{s})}{f_{R_1,R_2}(\boldsymbol{r})}$$

where $f_{R_1,R_2|S_1,S_2}(\boldsymbol{r}|\boldsymbol{s})$ is the conditional PDF of $\boldsymbol{r}$ given $\boldsymbol{s}$ and $P((S_1, S_2) = \boldsymbol{s})$ is the a priori probability that the pair $\boldsymbol{s}$ was transmitted. Hence, $P((S_1, S_2) = \boldsymbol{s}) = p_{U_1,U_2}(c(s_1), c(s_2))$, where $c(\,\cdot\,)$ is the constellation mapping function, which takes transmission signals and maps them to binary digits, i.e., $c(s_{ij}) = j$, for $i \in \{1, 2\}$ and $j \in \{0, 1\}$. Further, $f_{R_1,R_2}(\boldsymbol{r})$ is the pdf of the received values; however, having no dependence on $\boldsymbol{s}$ this term has no effect on the maximization, and can be dropped. Thus,

$$\hat{\boldsymbol{s}} = \operatorname*{arg\,max}_{\boldsymbol{s}\in\mathcal{S}_1\times\mathcal{S}_2} f_{R_1,R_2|S_1,S_2}(\boldsymbol{r}|\boldsymbol{s}) p_{U_1,U_2}(c(s_1), c(s_2)).$$

Recall that the AWGN terms N_1 and N_2 are independent. Consequently, given s_1, and s_2, R_1 and R_2 are conditionally independent. Thus, from the above

$$\begin{aligned}
\hat{\boldsymbol{s}} &= \operatorname*{arg\,max}_{\boldsymbol{s}\in\mathcal{S}_1\times\mathcal{S}_2} e^{-\frac{(r_1-s_1)^2}{2\sigma_1^2}-\frac{(r_2-s_2)^2}{2\sigma_2^2}} p_{U_1,U_2}(c(s_1), c(s_2)) \\
&= \operatorname*{arg\,max}_{\boldsymbol{s}\in\mathcal{S}_1\times\mathcal{S}_2} e^{-\frac{(r_1-s_1)^2}{2\sigma_1^2}} e^{-\frac{(r_2-s_2)^2}{2\sigma_2^2}} p_{U_1,U_2}(c(s_1), c(s_2)).
\end{aligned}$$

Further, taking the natural logarithm, a strictly increasing function, of the above expression, we obtain

$$\begin{aligned}
\hat{\boldsymbol{s}} &= \operatorname*{arg\,max}_{\boldsymbol{s}\in\mathcal{S}_1\times\mathcal{S}_2} \ln\left[e^{-\frac{(r_1-s_1)^2}{2\sigma_1^2}} e^{-\frac{(r_2-s_2)^2}{2\sigma_2^2}} p_{U_1,U_2}(c(s_1), c(s_2))\right] \\
&= \operatorname*{arg\,max}_{\boldsymbol{s}\in\mathcal{S}_1\times\mathcal{S}_2} \left[\ln p_{U_1,U_2}(c(s_1), c(s_2)) - \frac{r_1^2 + s_1^2 - 2r_1 s_1}{2\sigma_1^2} - \frac{r_2^2 + s_2^2 - 2r_2 s_2}{2\sigma_1^2}\right].
\end{aligned}$$

Lastly, the terms r_1^2 and r_2^2 do no influence the maximization and so can be dropped. Thus,

$$\hat{\boldsymbol{s}} = \operatorname*{arg\,max}_{\boldsymbol{s}\in\mathcal{S}_1\times\mathcal{S}_2} \left[\ln p_{U_1,U_2}(c(s_1), c(s_2)) - \frac{s_1^2 - 2r_1 s_1}{2\sigma_1^2} - \frac{s_2^2 - 2r_2 s_2}{2\sigma_1^2}\right] \tag{3.2}$$

is the MAP detection rule. We note that $s_1^2 = E_{1i}$ and $s_2^2 = E_{2j}$, the energies of the respective signals, where $i, j \in \{0, 1\}$.

3.5 Probability of Error

Using the MAP detection rule derived in the previous section, we now determine the probability of symbol error. Let e denote the error event, i.e., the event that $\hat{\boldsymbol{s}} = (\hat{s}_1, \hat{s}_2) \neq (s_1, s_2) = \boldsymbol{s}$. We are interested in determining $P(e) = \Pr\{\hat{\boldsymbol{s}} \neq \boldsymbol{s}\} = 1 - \Pr\{\hat{\boldsymbol{s}} = \boldsymbol{s}\}$, which from Bayes' rule can be written as

$$P(e) = 1 - \sum_{\boldsymbol{s} \in \mathcal{S}_1 \times \mathcal{S}_2} P(\hat{\boldsymbol{s}} = \boldsymbol{s} | \boldsymbol{s}) P(\boldsymbol{s}) \tag{3.3}$$

where $P(\hat{\boldsymbol{s}} = \boldsymbol{s}|\boldsymbol{s})$ is the probability of correct detection given that $\boldsymbol{s} \in \mathcal{S}_1 \times \mathcal{S}_2$ was sent and $P(\boldsymbol{s})$ is the a priori probability of the pair contained in $\boldsymbol{s}$. We wish to write $P(\hat{\boldsymbol{s}} = \boldsymbol{s}|\boldsymbol{s})$ in terms of the MAP decision rule. Let

$$h(\boldsymbol{s}) = h(s_1, s_2) = \ln p_{U_1,U_2}(c(s_1), c(s_2)) - \frac{s_1^2 - 2R_1 s_1}{2\sigma_1^2} - \frac{s_2^2 - 2R_2 s_2}{2\sigma_2^2}$$

(note that since $R_i = s_i + N_i$ for $i = 1, 2$, $h(\boldsymbol{s})$ is a random variable). Now let us consider the case when $\boldsymbol{s} = (s_{10}, s_{20})$, then

$$P(\hat{\boldsymbol{s}} = \boldsymbol{s} | \boldsymbol{s} = (s_{10}, s_{20})) = P\left(h(s_{10}, s_{20}) = \max_{(s_1,s_2) \in \mathcal{S}_1 \times \mathcal{S}_2} h(s_1, s_2) \middle| \boldsymbol{s} = (s_{10}, s_{20}) \right).$$

However, it will be convenient to express the above probability without the 'max' operation. Consider,

$$\begin{aligned} P&\left(h(s_{10}, s_{20}) = \max_{(s_1,s_2)} h(s_1, s_2) \middle| \boldsymbol{s} = (s_{10}, s_{20}) \right) \\ &= P\Bigg(h(s_{10}, s_{20}) \geq h(s_{11}, s_{20}), \\ &\qquad\qquad h(s_{10}, s_{20}) \geq h(s_{11}, s_{21}), \end{aligned}$$

$$
\begin{aligned}
&\qquad\qquad h(s_{10}, s_{20}) \geq h(s_{10}, s_{21}) \Big| \boldsymbol{s} = (s_{10}, s_{20})\Big) \\
&= P\Big(h(s_{11}, s_{20}) - h(s_{10}, s_{20}) \leq 0, \\
&\qquad h(s_{11}, s_{21}) - h(s_{10}, s_{20}) \leq 0, \\
&\qquad\qquad h(s_{10}, s_{21}) - h(s_{10}, s_{20}) \leq 0 \Big| \boldsymbol{s} = (s_{10}, s_{20})\Big).
\end{aligned}
$$

Note that $h(s_1, s_2)$ will follow a Gaussian distribution since N_1 and N_2 are Gaussian. The difference $h(\boldsymbol{s}) - h(\boldsymbol{t})$ where $\boldsymbol{s}, \boldsymbol{t} \in \mathcal{S}_1 \times \mathcal{S}_2$ such that $\boldsymbol{s} \neq \boldsymbol{t}$ will also be Gaussian. Letting,

$$X_1 = h(s_{11}, s_{20}) - h(s_{10}, s_{20}) \tag{3.4}$$

$$X_2 = h(s_{11}, s_{21}) - h(s_{10}, s_{20}) \tag{3.5}$$

$$X_3 = h(s_{10}, s_{21}) - h(s_{10}, s_{20}). \tag{3.6}$$

yields

$$
\begin{aligned}
X_1 &= \ln p_{U_1,U_2}(c(s_{11}), c(s_{20})) - \frac{E_{11} - 2R_1 s_{11}}{2\sigma_1^2} - \frac{E_{20} - 2R_2 s_{20}}{2\sigma_2^2} \\
&\quad - \left[\ln p_{U_1,U_2}(c(s_{10}), c(s_{20})) - \frac{E_{10} - 2R_1 s_{10}}{2\sigma_1^2} - \frac{E_{20} - 2R_2 s_{20}}{2\sigma_2^2} \right] \\
&= \ln \frac{p_{U_1,U_2}(c(s_{11}), c(s_{20}))}{p_{U_1,U_2}(c(s_{10}), c(s_{20}))} + \frac{E_{10} + 2R_1 s_{11} - E_{11} - 2R_1 s_{10}}{2\sigma_1^2} \\
&= \ln \frac{p_{U_1,U_2}(c(s_{11}), c(s_{20}))}{p_{U_1,U_2}(c(s_{10}), c(s_{20}))} + \frac{E_{10} - E_{11} + 2(s_{11} - s_{10})R_1}{2\sigma_1^2} \\
&= \ln \frac{p_{U_1,U_2}(c(s_{11}), c(s_{20}))}{p_{U_1,U_2}(c(s_{10}), c(s_{20}))} + \frac{E_{10} - E_{11}}{2\sigma_1^2} + \frac{s_{11} - s_{10}}{\sigma_1^2} R_1
\end{aligned}
$$

where $R_1 = s_{10} + N_1$ follows a $N(s_{10}, \sigma_1^2)$ distribution, where $N(a,b)$ denotes a Gaussian random variable with mean a and variance b, since $\boldsymbol{s} = (s_{10}, s_{20})$. Thus,

$$\begin{aligned}
\mu_{X_1} &= E[X_1] = \ln \frac{p_{U_1,U_2}(c(s_{11}), c(s_{20}))}{p_{U_1,U_2}(c(s_{10}), c(s_{20}))} + \frac{E_{10} - E_{11}}{2\sigma_1^2} + \frac{s_{11} - s_{10}}{\sigma_1^2} s_{10}, \\
\sigma_{X_1}^2 &= \mathrm{Var}(X_1) = \left(\frac{s_{10} - s_{11}}{\sigma_1^2} \right)^2 \mathrm{Var}(R_1) = \frac{(s_{11} - s_{10})^2}{\sigma_1^2}.
\end{aligned}$$

Hence, X_1 follows a $N(\mu_{X_1}, \sigma_{X_1}^2)$ distribution. A similar calculation shows X_3 follows a $N(\mu_{X_3}, \sigma_{X_3}^2)$ distribution where

$$\begin{aligned}
\mu_{X_3} &= E[X_3] = \ln \frac{p_{U_1,U_2}(c(s_{10}), c(s_{21}))}{p_{U_1,U_2}(c(s_{10}), c(s_{20}))} + \frac{E_{20} - E_{21}}{2\sigma_2^2} + \frac{s_{21} - s_{20}}{\sigma_2^2} s_{20}, \\
\sigma_{X_3}^2 &= \mathrm{Var}(X_3) = \left(\frac{s_{20} - s_{21}}{\sigma_2^2} \right)^2 \mathrm{Var}(R_2) = \frac{(s_{21} - s_{20})^2}{\sigma_2^2}.
\end{aligned}$$

Now, X_2 can be expressed in terms of X_1 and X_3. Indeed,

$$\begin{aligned}
X_2 &= \ln p_{U_1,U_2}(c(s_{11}), c(s_{21})) - \frac{E_{11} - 2R_1 s_{11}}{2\sigma_1^2} - \frac{E_{21} - 2R_2 s_{21}}{2\sigma_2^2} \\
&\quad - \left[\ln p_{U_1,U_2}(c(s_{10}), c(s_{20})) - \frac{E_{10} - 2R_1 s_{10}}{2\sigma_1^2} - \frac{E_{20} - 2R_2 s_{20}}{2\sigma_2^2} \right] \\
&= \ln \frac{p_{U_1,U_2}(c(s_{11}), c(s_{21}))}{p_{U_1,U_2}(c(s_{10}), c(s_{20}))} + \frac{E_{10} - E_{11}}{2\sigma_1^2} + \frac{E_{20} - E_{21}}{2\sigma_2^2} \\
&\quad + \frac{s_{11} - s_{10}}{\sigma_1^2} R_1 + \frac{s_{21} - s_{20}}{\sigma_2^2} R_2 \\
&= \ln \frac{p_{U_1,U_2}(c(s_{11}), c(s_{21}))}{p_{U_1,U_2}(c(s_{10}), c(s_{20}))} + \frac{E_{10} - E_{11}}{2\sigma_1^2} + \frac{E_{20} - E_{21}}{2\sigma_2^2} \\
&\quad + \frac{s_{11} - s_{10}}{\sigma_1^2} R_1 + \frac{s_{21} - s_{20}}{\sigma_2^2} R_2 \\
&= \ln \frac{p_{U_1,U_2}(c(s_{11}), c(s_{20}))}{p_{U_1,U_2}(c(s_{10}), c(s_{20}))} + \frac{E_{10} - E_{11}}{2\sigma_1^2} + \frac{s_{11} - s_{10}}{\sigma_1^2} R_1 - \ln \frac{p_{U_1,U_2}(c(s_{11}), c(s_{20}))}{p_{U_1,U_2}(c(s_{10}), c(s_{20}))} \\
&\quad + \ln \frac{p_{U_1,U_2}(c(s_{10}), c(s_{21}))}{p_{U_1,U_2}(c(s_{10}), c(s_{20}))} + \frac{E_{20} - E_{21}}{2\sigma_2^2} + \frac{s_{21} - s_{20}}{\sigma_2^2} R_2 \\
&\qquad - \ln \frac{p_{U_1,U_2}(c(s_{10}), c(s_{21}))}{p_{U_1,U_2}(c(s_{10}), c(s_{20}))} + \ln \frac{p_{U_1,U_2}(c(s_{11}), c(s_{21}))}{p_{U_1,U_2}(c(s_{10}), c(s_{20}))}
\end{aligned}$$

$$
\begin{aligned}
&= X_1 - \ln \frac{p_{U_1,U_2}(c(s_{11}), c(s_{20}))}{p_{U_1,U_2}(c(s_{10}), c(s_{20}))} + X_3 - \ln \frac{p_{U_1,U_2}(c(s_{10}), c(s_{21}))}{p_{U_1,U_2}(c(s_{10}), c(s_{20}))} \\
&\quad + \ln \frac{p_{U_1,U_2}(c(s_{11}), c(s_{21}))}{p_{U_1,U_2}(c(s_{10}), c(s_{20}))} \\
&= X_1 + X_3 - \ln p_{U_1,U_2}(c(s_{11}), c(s_{20})) + \ln p_{U_1,U_2}(c(s_{10}), c(s_{20})) \\
&\qquad - \ln p_{U_1,U_2}(c(s_{10}), c(s_{21})) + \ln p_{U_1,U_2}(c(s_{10}), c(s_{20})) \\
&\qquad + \ln p_{U_1,U_2}(c(s_{11}), c(s_{21})) - \ln p_{U_1,U_2}(c(s_{10}), c(s_{20})) \\
&= X_1 + X_3 + \ln \frac{p_{U_1,U_2}(c(s_{10}), c(s_{20})) p_{U_1,U_2}(c(s_{11}), c(s_{21}))}{p_{U_1,U_2}(c(s_{11}), c(s_{20})) p_{U_1,U_2}(c(s_{10}), c(s_{21}))}
\end{aligned}
$$

To ease notation let

$$
\alpha = \ln \frac{p_{U_1,U_2}(c(s_{10}), c(s_{20})) p_{U_1,U_2}(c(s_{11}), c(s_{21}))}{p_{U_1,U_2}(c(s_{11}), c(s_{20})) p_{U_1,U_2}(c(s_{10}), c(s_{21}))}. \tag{3.7}
$$

Thus,

$$
\begin{aligned}
P(\hat{\boldsymbol{s}} = \boldsymbol{s} | \boldsymbol{s} = (s_{10}, s_{20})) &= P\left(h(s_{10}, s_{20}) = \max_{(s_1,s_2)} h(s_1, s_2) \middle| \boldsymbol{s} = (s_{10}, s_{20}) \right) \\
&= P(X_1 \leq 0, X_2 \leq 0, X_3 \leq 0 | \boldsymbol{s} = (s_{10}, s_{20})) \\
&= P(X_1 \leq 0, X_1 + X_3 + \alpha \leq 0, X_3 \leq 0 | \boldsymbol{s} = (s_{10}, s_{20})).
\end{aligned}
$$

For $\alpha > 0$ the joint event $\{X_1 \leq 0, X_1 + X_3 + \alpha \leq 0, X_3 \leq 0 | \boldsymbol{s} = (s_{10}, s_{20})\}$ can be represented as a region in the (x_1, x_3)-plane as shown in the Figure 3.5. Thus,

$$
\begin{aligned}
&P(X_1 < 0, X_1 + X_3 + \alpha < 0, X_3 < 0 | \boldsymbol{s} = (s_{10}, s_{20})) \\
&\quad = \int_{-\infty}^{0} \int_{-\infty}^{0} f_{X_1,X_3}(x_1, x_3) dx_1 dx_3 - \int_{-\alpha}^{0} \int_{-x_3-\alpha}^{0} f_{X_1,X_3}(x_1, x_3) dx_1 dx_3.
\end{aligned}
$$

where $f_{X_1,X_3}(x_1, x_3)$ is the joint pdf of X_1 and X_3. To determine this density, we note X_1 and X_3 are independent since X_1 and X_3 are functions of the independent

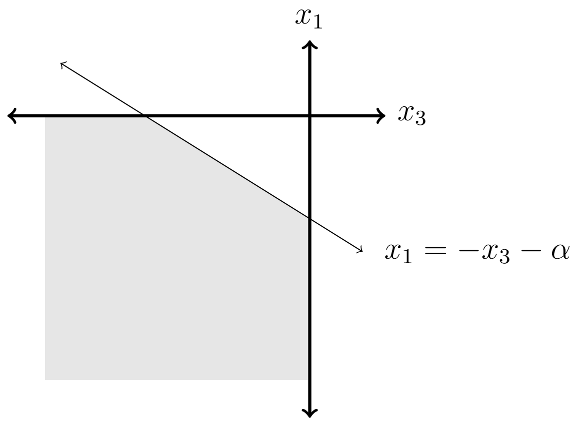

Figure 3.5: Error event when $\boldsymbol{s} = (s_{10}, s_{20})$ in the (x_1, x_3)-plane.

random variables N_1 and N_2, respectively. Hence

$$f_{X_1,X_3}(x_1, x_3) = \frac{1}{2\pi\sigma_{X_1}\sigma_{X_3}} \exp\left\{-\frac{1}{2}\left[\frac{(x_1 - \mu_{X_1})^2}{\sigma_{X_1}^2} + \frac{(x_3 - \mu_{X_3})^2}{\sigma_{X_3}^2}\right]\right\}.$$

As a final step step, since X_1 and X_3 are independent and letting

$$\Delta_X = \int_{-\alpha}^{0}\int_{-x_3-\alpha}^{0} f_{X_1,X_3}(x_1, x_3)dx_1dx_3,$$

we write

$$P(\hat{\boldsymbol{s}} = \boldsymbol{s}|\boldsymbol{s} = (s_{10}, s_{20})) = Q\left(\frac{\mu_{X_1}}{\sigma_{X_1}}\right) Q\left(\frac{\mu_{X_3}}{\sigma_{X_3}}\right) - \Delta_X. \tag{3.8}$$

Note that if $-\alpha > 0$, then $\Delta_X = 0$. When $\boldsymbol{s} = (s_{11}, s_{21})$, $\boldsymbol{s} = (s_{10}, s_{21})$, and $\boldsymbol{s} = (s_{11}, s_{20})$ the results are analogous to those above. A summary is presented below:

Case 1: $\boldsymbol{s} = (s_{11}, s_{21})$

In this case (3.8) is written as

$$P(\hat{\boldsymbol{s}} = \boldsymbol{s}|\boldsymbol{s} = (s_{11}, s_{21})) = Q\left(\frac{\mu_{Y_1}}{\sigma_{Y_1}}\right) Q\left(\frac{\mu_{Y_3}}{\sigma_{Y_3}}\right) - \Delta_Y$$

where

$$\begin{aligned}
\mu_{Y_1} &= E[Y_1] = \ln\frac{p_{U_1,U_2}(c(s_{10}), c(s_{21}))}{p_{U_1,U_2}(c(s_{11}), c(s_{21}))} + \frac{E_{11} - E_{10}}{2\sigma_1^2} + \frac{s_{10} - s_{11}}{\sigma_1^2}s_{11} \\
\mu_{Y_3} &= E[Y_3] = \ln\frac{p_{U_1,U_2}(c(s_{11}), c(s_{20}))}{p_{U_1,U_2}(c(s_{11}), c(s_{21}))} + \frac{E_{21} - E_{20}}{2\sigma_2^2} + \frac{s_{20} - s_{21}}{\sigma_2^2}s_{21} \\
\sigma_{Y_1}^2 &= \mathrm{Var}(Y_1) = \frac{(s_{10} - s_{11})^2}{\sigma_1^2} \\
\sigma_{Y_3}^2 &= \mathrm{Var}(Y_3) = \frac{(s_{20} - s_{21})^2}{\sigma_2^2}
\end{aligned}$$

and

$$\Delta_Y = \begin{cases} \int_{-\alpha}^{0}\int_{-y_3-\alpha}^{0} f_{Y_1,Y_3}(y_1, y_3)dy_1dy_3 \text{ if } \alpha > 0 \\ 0 \text{ otherwise} \end{cases}$$

where

$$f_{Y_1,Y_3}(y_1, y_3) = \frac{1}{2\pi\sigma_{Y_1}\sigma_{Y_3}} \exp\left\{-\frac{1}{2}\left[\frac{(y_1 - \mu_{Y_1})^2}{\sigma_{Y_1}^2} + \frac{(y_3 - \mu_{Y_3})^2}{\sigma_{Y_3}^2}\right]\right\}.$$

Case 2: $\boldsymbol{s} = (s_{10}, s_{21})$

In this case (3.8) is written as

$$P(\hat{\boldsymbol{s}} = \boldsymbol{s}|\boldsymbol{s} = (s_{10}, s_{21})) = Q\left(\frac{\mu_{Z_1}}{\sigma_{Z_1}}\right) Q\left(\frac{\mu_{Z_3}}{\sigma_{Z_3}}\right) - \Delta_Z$$

where

$$\mu_{Z_1} = E[Z_1] = \ln \frac{p_{U_1,U_2}(c(s_{11}), c(s_{21}))}{p_{U_1,U_2}(c(s_{10}), c(s_{21}))} + \frac{E_{10} - E_{11}}{2\sigma_1^2} + \frac{s_{11} - s_{10}}{\sigma_1^2} s_{10}$$
$$\mu_{Z_3} = E[Z_3] = \ln \frac{p_{U_1,U_2}(c(s_{10}), c(s_{20}))}{p_{U_1,U_2}(c(s_{10}), c(s_{21}))} + \frac{E_{21} - E_{20}}{2\sigma_2^2} + \frac{s_{20} - s_{21}}{\sigma_2^2} s_{21}$$
$$\sigma_{Z_1}^2 = \mathrm{Var}(Z_1) = \frac{(s_{11} - s_{10})^2}{\sigma_1^2}$$
$$\sigma_{Z_3}^2 = \mathrm{Var}(Z_3) = \frac{(s_{20} - s_{21})^2}{\sigma_2^2}$$

and

$$\Delta_Z = \begin{cases} \int_\alpha^0 \int_{-z_3+\alpha}^0 f_{Z_1,Z_3}(z_1, z_3) dz_1 dz_3 \text{ if } \alpha < 0 \\ 0 \text{ otherwise} \end{cases}$$

where

$$f_{Z_1,Z_3}(z_1, z_3) = \frac{1}{2\pi\sigma_{Z_1}\sigma_{Z_3}} \exp\left\{-\frac{1}{2}\left[\frac{(z_1 - \mu_{Z_1})^2}{\sigma_{Z_1}^2} + \frac{(z_3 - \mu_{Z_3})^2}{\sigma_{Z_3}^2}\right]\right\}.$$

See Appendix A for an explanation on why $\Delta_Z = 0$ for $\alpha > 0$ as opposed to $\Delta_X = \Delta_Y = 0$ if $\alpha \leq 0$.

Case 3: $\boldsymbol{s} = (s_{11}, s_{20})$

In this case (3.8) is written as

$$P(\hat{\boldsymbol{s}} = \boldsymbol{s} | \boldsymbol{s} = (s_{11}, s_{20})) = Q\left(\frac{\mu_{W_1}}{\sigma_{W_1}}\right) Q\left(\frac{\mu_{W_3}}{\sigma_{W_3}}\right) - \Delta_W$$

where

$$\mu_{W_1} = E[W_1] = \ln \frac{p_{U_1,U_2}(c(s_{10}), c(s_{20}))}{p_{U_1,U_2}(c(s_{11}), c(s_{20}))} + \frac{E_{11} - E_{10}}{2\sigma_1^2} + \frac{s_{10} - s_{11}}{\sigma_1^2} s_{11}$$

$$
\begin{aligned}
\mu_{W_3} &= E[W_3] = \ln \frac{p_{U_1,U_2}(c(s_{11}), c(s_{21}))}{p_{U_1,U_2}(c(s_{11}), c(s_{20}))} + \frac{E_{20} - E_{21}}{2\sigma_2^2} + \frac{s_{21} - s_{20}}{\sigma_2^2} s_{20} \\
\sigma_{W_1}^2 &= \mathrm{Var}(W_1) = \frac{(s_{10} - s_{11})^2}{\sigma_1^2} \\
\sigma_{W_3}^2 &= \mathrm{Var}(W_3) = \frac{(s_{21} - s_{20})^2}{\sigma_2^2}
\end{aligned}
$$

and

$$
\Delta_W = \begin{cases} \int_{\alpha}^{0} \int_{-w_3+\alpha}^{0} f_{W_1,W_3}(w_1, w_3) dw_1 dw_3 \text{ if } \alpha < 0 \\ 0 \text{ otherwise} \end{cases}
$$

where

$$
f_{W_1,W_3}(w_1, w_3) = \frac{1}{2\pi\sigma_{W_1}\sigma_{W_3}} \exp\left\{ -\frac{1}{2} \left[\frac{(w_1 - \mu_{W_1})^2}{\sigma_{W_1}^2} + \frac{(w_3 - \mu_{W_3})^2}{\sigma_{W_3}^2} \right] \right\}.
$$

Again, see Appendix A for the sign change in α.

Finally, the probability of error as seen in (3.3) is given as

$$
\begin{aligned}
P(e) = 1 &- \left[Q\left(\frac{\mu_{X_1}}{\sigma_{X_1}}\right) Q\left(\frac{\mu_{X_3}}{\sigma_{X_3}}\right) - \Delta_X \right] p_{U_1,U_2}(c(s_{10}), c(s_{20})) \\
&- \left[Q\left(\frac{\mu_{Y_1}}{\sigma_{Y_1}}\right) Q\left(\frac{\mu_{Y_3}}{\sigma_{Y_3}}\right) - \Delta_Y \right] p_{U_1,U_2}(c(s_{11}), c(s_{21})) \\
&- \left[Q\left(\frac{\mu_{Z_1}}{\sigma_{Z_1}}\right) Q\left(\frac{\mu_{Z_3}}{\sigma_{Z_3}}\right) - \Delta_Z \right] p_{U_1,U_2}(c(s_{10}), c(s_{21})) \\
&- \left[Q\left(\frac{\mu_{W_1}}{\sigma_{W_1}}\right) Q\left(\frac{\mu_{W_3}}{\sigma_{W_3}}\right) - \Delta_W \right] p_{U_1,U_2}(c(s_{11}), c(s_{20})). \qquad (3.9)
\end{aligned}
$$

Remark: Letting $p_1 = p_2 = p$, $p_{11} = (1-p)^2$, $E_1 = E_2$, and $\gamma_1 = \gamma_2$ we have that

$$
\begin{aligned}
P(e) &= 1 - P(\hat{\boldsymbol{s}} = \boldsymbol{s}) \\
&= 1 - P(\hat{s}_1 = s_1, s_2 = s_2) \\
&= 1 - [P(\hat{s}_1 = s_1)]^2
\end{aligned}
$$

by the orthogonality of the channels and the symmetry of the transmitters and since in this case U_1 and U_2 become independendent of each other with identical distribution vector given by $(p, 1-p)$ (i.e., the two-dimensional source reduces to two independent Bernoulli(p) sources). From here the probability of error can be calculated as

$$\begin{aligned} P(e) &= 1 - [P(\hat{s}_1 = s_1)]^2 \\ &= 1 - [P(\hat{s}_1 = s_1 | s_1 = s_{11})P(s_1 = s_{11}) + P(\hat{s}_1 = s_1 | s_1 = s_{10})P(s_1 = s_{10})]^2 \\ &= 1 - [P(\hat{s}_1 = s_1 | s_1 = s_{11})(1-p) + P(\hat{s}_1 = s_1 | s_1 = s_{10})p]^2. \end{aligned}$$

Lastly, notice that $P(\hat{s}_1 = s_1 | s_1 = s_{11})(1-p) + P(\hat{s}_1 = s_1 | s_1 = s_{10})p$ is exactly the expression seen in (2.3), namely the BEP in [1].

3.6 Union Bound on the Probability of Error

From [2] the union bound gives

$$P(e) = \sum_{\boldsymbol{s} \in S_1 \times S_2} P(e|\boldsymbol{s})P(\boldsymbol{s}) \leq \sum_{\boldsymbol{s} \in S_1 \times S_2} \sum_{\tilde{\boldsymbol{s}} \neq \boldsymbol{s}} P(e_{\tilde{\boldsymbol{s}}\boldsymbol{s}})P(\boldsymbol{s}) = \sum_{\boldsymbol{s} \in S_1 \times S_2} P(\boldsymbol{s}) \sum_{\tilde{\boldsymbol{s}} \neq \boldsymbol{s}} P(e_{\tilde{\boldsymbol{s}}\boldsymbol{s}})$$

where for $\tilde{\boldsymbol{s}}, \boldsymbol{s} \in \mathcal{S}_1 \times \mathcal{S}_2$, $e_{\tilde{\boldsymbol{s}}\boldsymbol{s}}$ is the event that $\tilde{\boldsymbol{s}}$ has a higher MAP metric than $\boldsymbol{s}$, given that $\boldsymbol{s}$ was transmitted, i.e.,

$$P(e_{\tilde{\boldsymbol{s}}\boldsymbol{s}}) = P(h(\tilde{\boldsymbol{s}}) > h(\boldsymbol{s})).$$

Now, letting $\boldsymbol{s} = (s_{10}, s_{20})$, we have

$$\sum_{\tilde{\boldsymbol{s}} \neq \boldsymbol{s}} P(e_{\tilde{\boldsymbol{s}}\boldsymbol{s}}) = P(h(s_{11}, s_{20}) > h(s_{10}, s_{20}))$$

$$
\begin{aligned}
&\quad + P(h(s_{11}, s_{21}) > h(s_{10}, s_{20})) \\
&\qquad + P(h(s_{10}, s_{21}) > h(s_{10}, s_{20})) \\
&= 1 - P(h(s_{11}, s_{20}) - h(s_{10}, s_{20}) < 0) \\
&\quad + 1 - P(h(s_{11}, s_{21}) - h(s_{10}, s_{20}) < 0) \\
&\qquad + 1 - P(h(s_{10}, s_{21}) - h(s_{10}, s_{20}) < 0) \\
&= 1 - P(X_1 < 0) + 1 - P(X_2 < 0) + 1 - P(X_3 < 0) \qquad (3.10)
\end{aligned}
$$

where X_1, X_2, and X_3 are as before, given in (3.4), (3.5), and (3.5), respectively. Recall that $X_2 = X_1 + X_3 + \alpha$, where X_1 and X_3 are independent. Thus,

$$
\begin{aligned}
P(X_1 < 0) &= Q\left(\frac{\mu_{X_1}}{\sigma_{X_1}}\right) \\
P(X_3 < 0) &= Q\left(\frac{\mu_{X_3}}{\sigma_{X_3}}\right).
\end{aligned}
$$

Further,

$$
P(X_2 < 0) = Q\left(\frac{\mu_{X_1} + \mu_{X_3} + \alpha_X}{\sqrt{\sigma_{X_1}^2 + \sigma_{X_3}^2}}\right)
$$

since

$$
E[X_1 + X_3 + \alpha] = E[X_1] + E[X_3] + \alpha = \mu_{X_1} + \mu_{X_3} + \alpha
$$

and

$$
\mathrm{Var}(X_2) = \mathrm{Var}(X_1 + X_3) = \mathrm{Var}(X_1) + \mathrm{Var}(X_3) = \sigma_{X_1}^2 + \sigma_{X_3}^2
$$

by independence of X_1 and X_3. Thus, we can write (3.10) as

$$
\sum_{\tilde{\boldsymbol{s}} \neq \boldsymbol{s}} P(e_{\tilde{\boldsymbol{s}}\boldsymbol{s}}) = \left(1 - Q\left(\frac{\mu_{X_1}}{\sigma_{X_1}}\right)\right) + \left(1 - Q\left(\frac{\mu_{X_1} + \mu_{X_3} + \alpha_X}{\sqrt{\sigma_{X_1}^2 + \sigma_{X_3}^2}}\right)\right) + \left(1 - Q\left(\frac{\mu_{X_3}}{\sigma_{X_2}}\right)\right)
$$

$$= 3 - Q\left(\frac{\mu_{X_1}}{\sigma_{X_1}}\right) - Q\left(\frac{\mu_{X_1} + \mu_{X_3} + \alpha_X}{\sqrt{\sigma_{X_1}^2 + \sigma_{X_3}^2}}\right) - Q\left(\frac{\mu_{X_3}}{\sigma_{X_2}}\right)$$

The cases for letting $\boldsymbol{s} = (s_{11}, s_{21})$, $\boldsymbol{s} = (s_{10}, s_{21})$, and $\boldsymbol{s} = (s_{11}, s_{20})$, are analogously derived. We obtain

$$\begin{aligned}
P(e) &= \sum_{\boldsymbol{s} \in S_1 \times S_2} P(e|\boldsymbol{s})P(\boldsymbol{s}) \\
&\leq \sum_{\boldsymbol{s} \in S_1 \times S_2} P(\boldsymbol{s}) \sum_{\tilde{\boldsymbol{s}} \neq \boldsymbol{s}} P(e_{\tilde{\boldsymbol{s}}\boldsymbol{s}}) \\
&= \left[3 - Q\left(\frac{\mu_{X_1}}{\sigma_{X_1}}\right) - Q\left(\frac{\mu_{X_1} + \mu_{X_3} + \alpha}{\sqrt{\sigma_{X_1}^2 + \sigma_{X_3}^2}}\right) - Q\left(\frac{\mu_{X_3}}{\sigma_{X_3}}\right)\right] P(c(s_{10}), c(s_{20})) \\
&\quad + \left[3 - Q\left(\frac{\mu_{Y_1}}{\sigma_{Y_1}}\right) - Q\left(\frac{\mu_{Y_1} + \mu_{Y_3} + \alpha}{\sqrt{\sigma_{Y_1}^2 + \sigma_{Y_3}^2}}\right) - Q\left(\frac{\mu_{Y_3}}{\sigma_{Y_3}}\right)\right] P(c(s_{11}), c(s_{21})) \\
&\quad + \left[3 - Q\left(\frac{\mu_{Z_1}}{\sigma_{Z_1}}\right) - Q\left(\frac{\mu_{Z_1} + \mu_{Z_3} - \alpha}{\sqrt{\sigma_{Z_1}^2 + \sigma_{Z_3}^2}}\right) - Q\left(\frac{\mu_{Z_3}}{\sigma_{Z_3}}\right)\right] P(c(s_{10}), c(s_{21})) \\
&\quad + \left[3 - Q\left(\frac{\mu_{W_1}}{\sigma_{W_1}}\right) - Q\left(\frac{\mu_{W_1} + \mu_{W_3} - \alpha}{\sqrt{\sigma_{W_1}^2 + \sigma_{W_3}^2}}\right) - Q\left(\frac{\mu_{W_3}}{\sigma_{W_3}}\right)\right] P(c(s_{11}), c(s_{20})).
\end{aligned} \tag{3.11}$$

Lastly, we will denote (3.11) as $P_{UB}(e)$.

Chapter 4

Optimization of Signal Energies and Numerical Results

4.1 Verification of Probability of Error Derivation

To confirm the validity of the probability of error result derived in Chapter 3, we will compare simulation results to error probabilities obtained from (3.9). We assume for Sections 4.1–4.4 that $\gamma_1 = \gamma_2 = \gamma \in \{-1, 1\}$. Moreover, we will include the union bound in the comparison. Consider the error probability plots when $\gamma = 1$ and $\gamma = -1$ in Figures 4.1 and 4.2 respectively. In this report we use the signal to noise ratio (SNR) defined in [6], namely

$$\text{SNR} = \frac{E_1 + E_2}{\sigma_1^2 + \sigma_2^2}. \tag{4.1}$$

For these simulations, 4×10^6 of source data pairs were transmitted, and $\sigma_1 = \sigma_2 = 2$, E_1 and E_2 were varied from 2 to 20. Further we used $p_1 = p_2 = 0.1$ and $\rho = 0.9$.

As one can see from Figures 4.1 and 4.2, the simulation and error probabilities obtained from (3.9) coincide. Also, as is expected the union bound, (3.11), provides a rather tight upper bound on the probability of error.

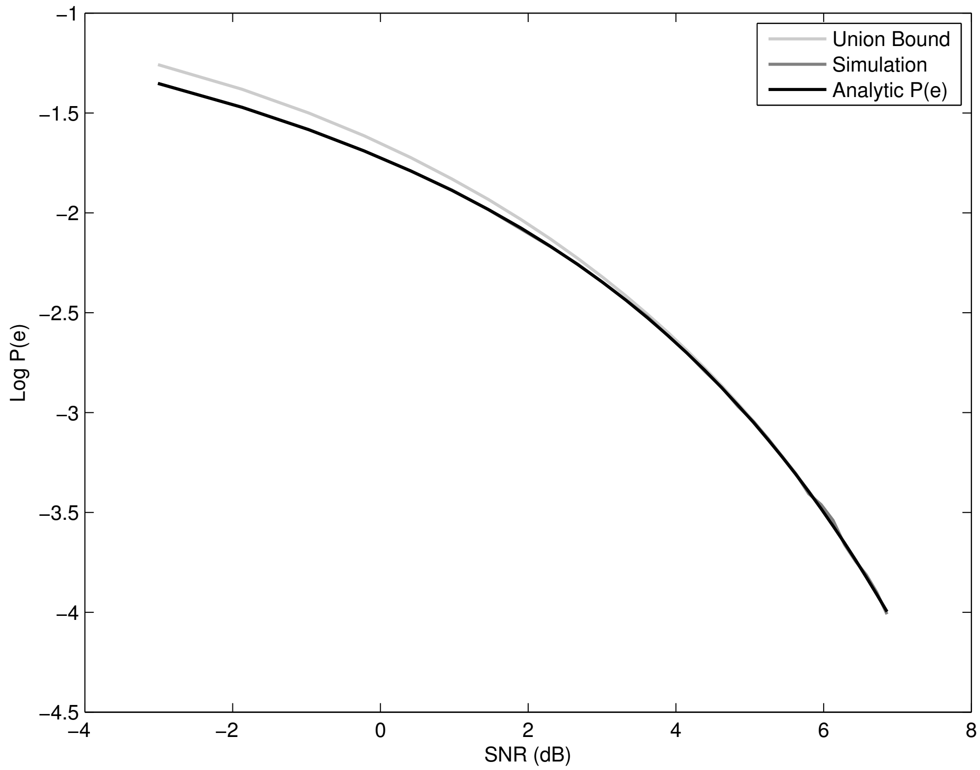

Figure 4.1: Error probability plots for $\gamma = 1$.

4.2 Numerical Optimization of E_{10} and E_{20}

At this point it seems unclear wether or not the optimal energy allocation, which minimize $P(e)$ (given in (3.9)) of our system will match [1]. On one hand the MAP detection depends on the correlation coefficient of the source sample pairs. On the other hand, the transmitters have no way of cooperating.

As a first step to optimization we consider numeric analysis of (3.9). For $\gamma = 1$, consider Figures 4.3 and 4.4, where we set $E_1 = E_2$ and $2E_1 = E_2$, respectively. For $\gamma = -1$, consider Figures 4.5 and 4.6 for cases $E_1 = E_2$ and $2E_1 = E_2$, respectively. In all four figures, '$*$' denotes the location of the numerically determined minimum. In all figures in this section we chose, $p_1 = p_2 = 0.1$, and $\rho = 0.9$. For Figures 4.3–4.6,

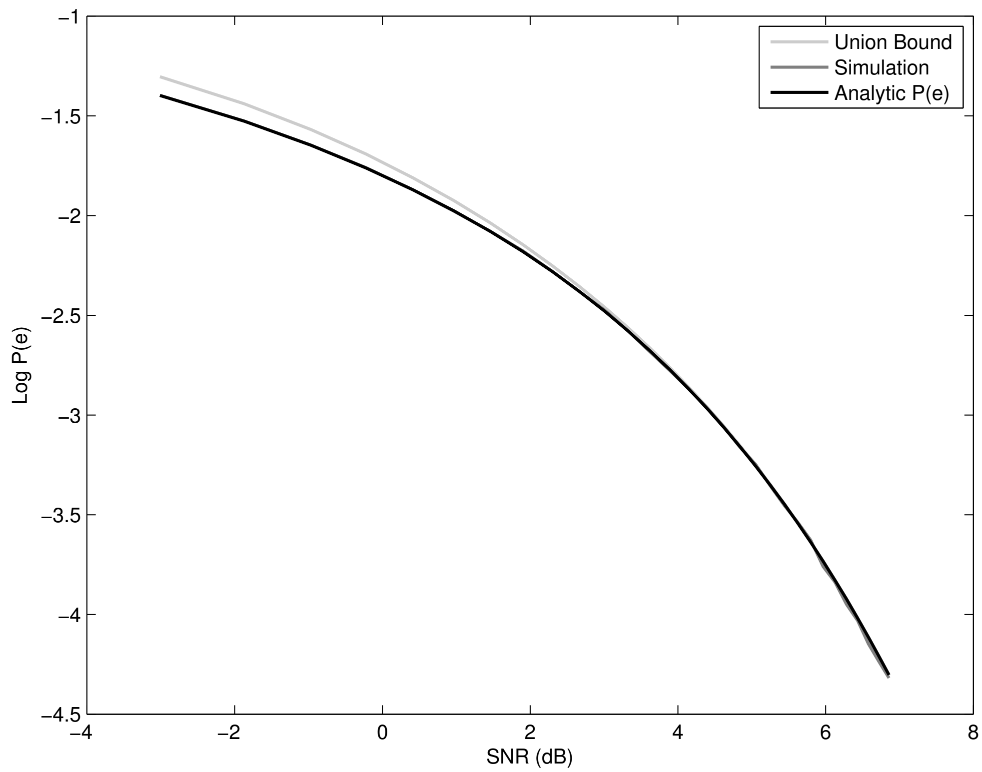

Figure 4.2: Error probability plots for $\gamma = -1$.

$\sigma_1 = \sigma_2 = 4$. For Figures 4.3 and 4.5, $E_1 = E_2 = 10$, whereas for Figures 4.4 and 4.6 $E_1 = 10$ and $E_2 = 20$. In Tables 4.1 and 4.2 we give a comparison of the results of [1] and our numerical experiments, for $\gamma = 1$ and $\gamma = -1$, respectively. From these tables we can deduce for these particular values that the optimal energies of our system coincide with the results from [1] (or see (2.5) and (2.6)–(2.7)). For a more complete picture consider, for $\gamma = 1$, Figures 4.7 and 4.8 corresponding to $E_1 = E_2$ and $2E_1 = E_2$, respectively, and for $\gamma = -1$, Figures 4.9 and 4.10 corresponding to $E_1 = E_2$ and $2E_1 = E_2$, respectively. For Figures 4.7-4.10, $E_1 \in [2, 20]$ and $\sigma_1 = \sigma_2 = 2$. These figures show the optimal values for E_{10} and E_{20} as functions of SNR. For comparison purposes we also plotted in Figures 4.7-4.10 the curves representing the analytic results from [1]. In Figures 4.7-4.10 we see that for all SNR

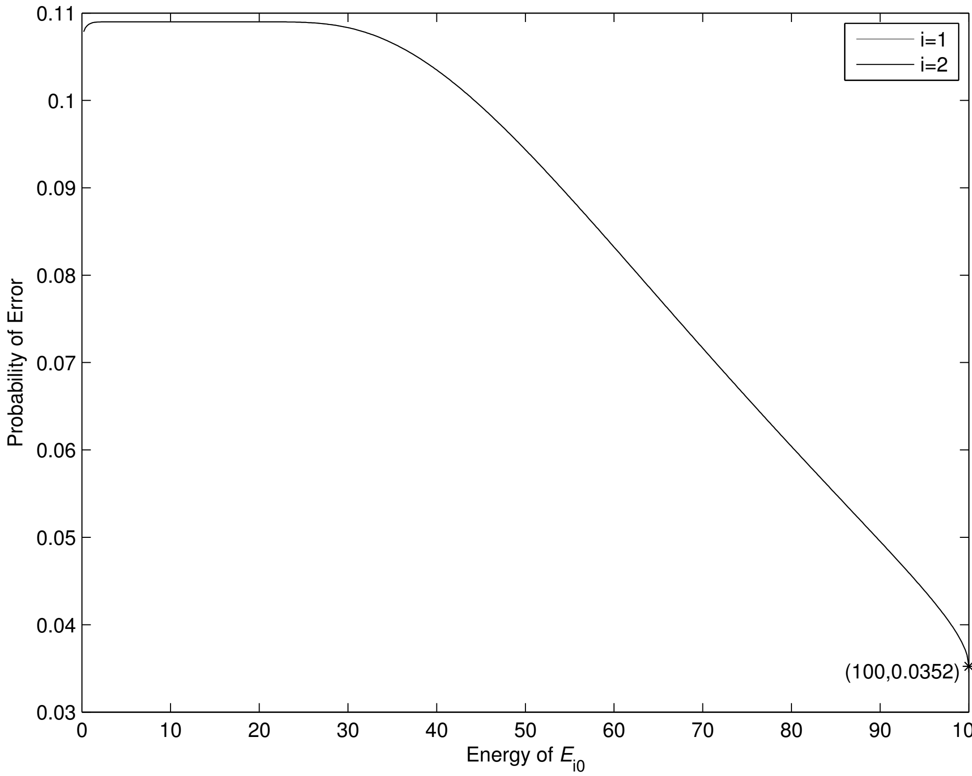

Figure 4.3: Numerical optimization when $\gamma = 1$ and $E_1 = E_2$.

	Numerically optimal E_{10}	E_{10} from [1]	Numerically optimal E_{20}	E_{20} from [1]
$\gamma = 1$	100	100	100	100
$\gamma = -1$	90	90	90	90

Table 4.1: Comparison of our numerical optimization results and [1] for E_{10} and E_{20} when $E_1 = E_2$.

values the optimal values for E_{10} and E_{20} coincide with the results from [1].

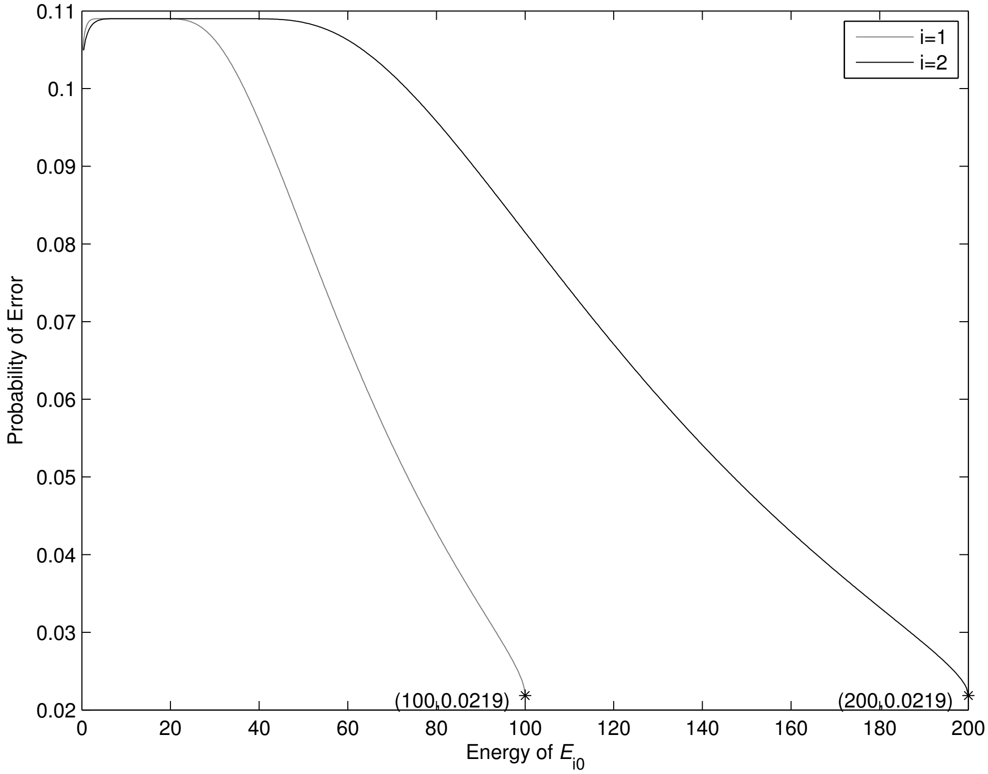

Figure 4.4: Numerical optimization when $\gamma = 1$ and $2E_1 = E_2$.

	Numerically optimal E_{10}	E_{10} from [1]	Numerically optimal E_{20}	E_{20} from [1]
$\gamma = 1$	100	100	200	200
$\gamma = -1$	90	90	180	180

Table 4.2: Comparison of our numerical optimization results and [1] for E_{10} and E_{20} when $2E_1 = E_2$.

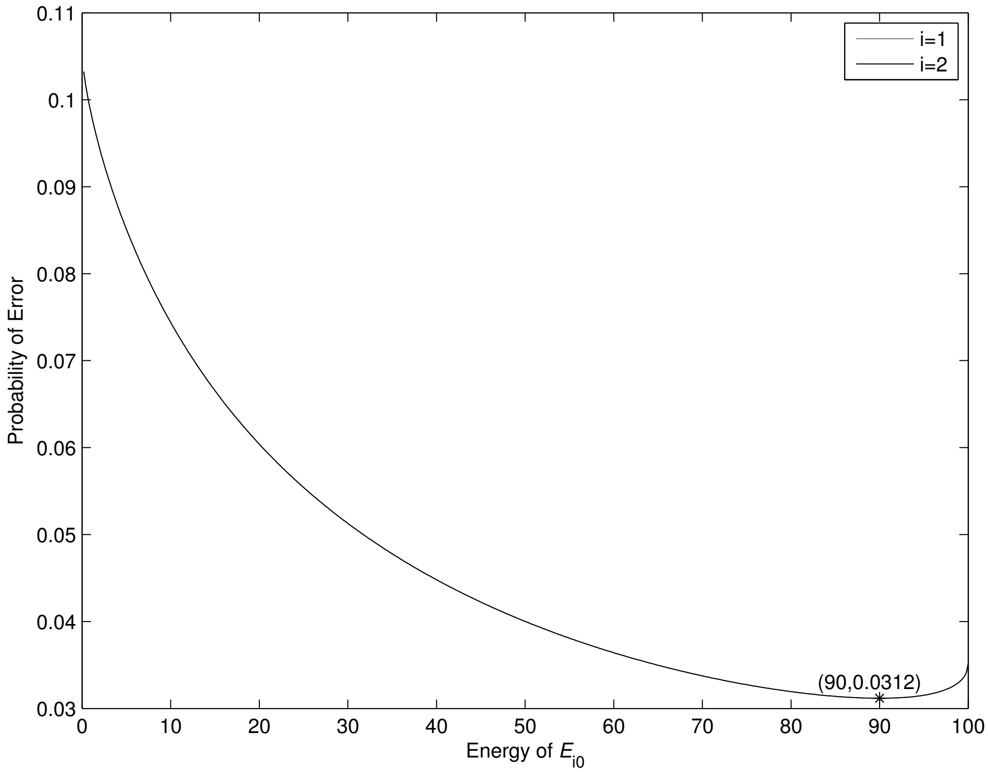

Figure 4.5: Numerical optimization when $\gamma = -1$ and $E_1 = E_2$.

4.3 Analytical Optimization of E_{10} and E_{20}

In the previous section it was numerically demonstrated that the optimal energies for E_{10} and E_{20} match the results of [1]. However, the terms Δ_V for $V = X, Y, Z, W$ in the probability of error expression (3.9) are hard to handle when analytical optimizing. To work around this, first we will show that $\lim_{\sigma_1,\sigma_2 \to 0} P_{UB}(e) = 0$, to verify (3.11) in the asymptotically high SNR regime. Then, we analytically optimize $P_{UB}(e)$.

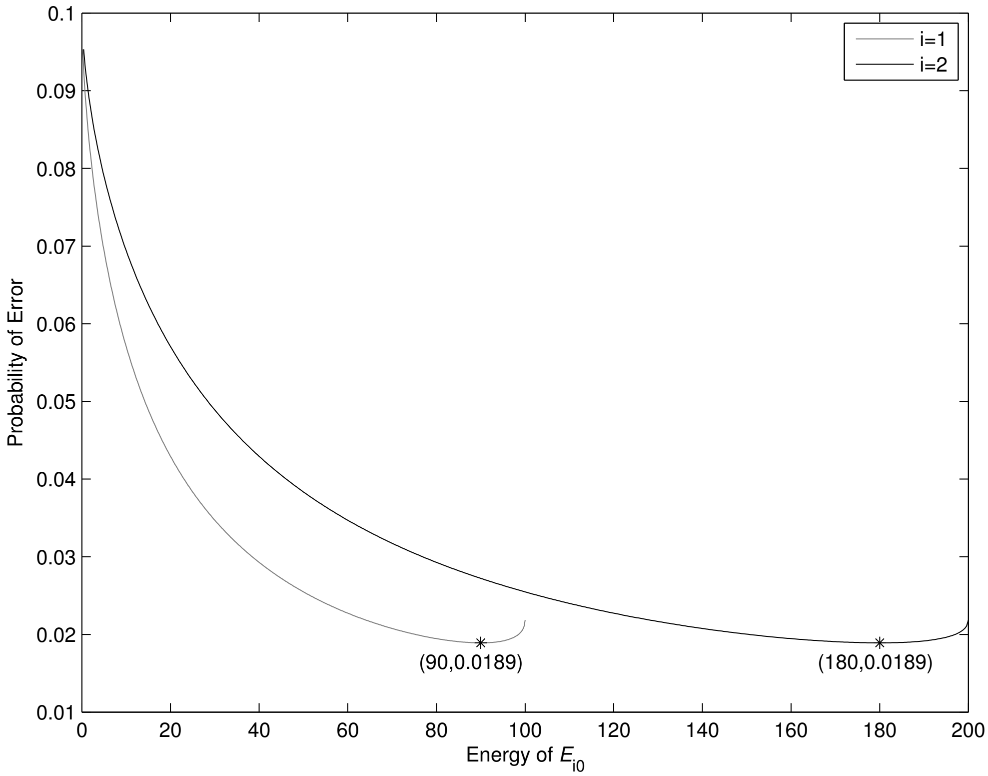

Figure 4.6: Numerical optimization when $\gamma = -1$ and $2E_1 = E_2$.

4.3.1 Union Error Bound Vanishes with Increasing SNR

Considering (3.11) and letting

$$\lambda_{X_1} = \ln[p_{U_1,U_2}(c(s_{11}), c(s_{20}))/p_{U_1,U_2}(c(s_{10}), c(s_{20}))]$$

we note

$$\frac{\mu_{X_1}}{\sigma_{X_1}} = \frac{\lambda_{X_1}\sigma_1}{\sqrt{(s_{11}-s_{10})^2}} + \frac{E_{10}-E_{11}}{2\sigma_1\sqrt{(s_{11}-s_{10})^2}} + \frac{s_{11}-s_{10}}{\sigma_1\sqrt{(s_{11}-s_{10})^2}}s_{10} \qquad (4.2)$$

where

$$s_{10} = \sqrt{E_{10}}\gamma,\ s_{11} = \sqrt{E_{11}},\ \text{and}\ E_{11} = \frac{E_1 - E_{10}p_1}{1-p_1}.$$

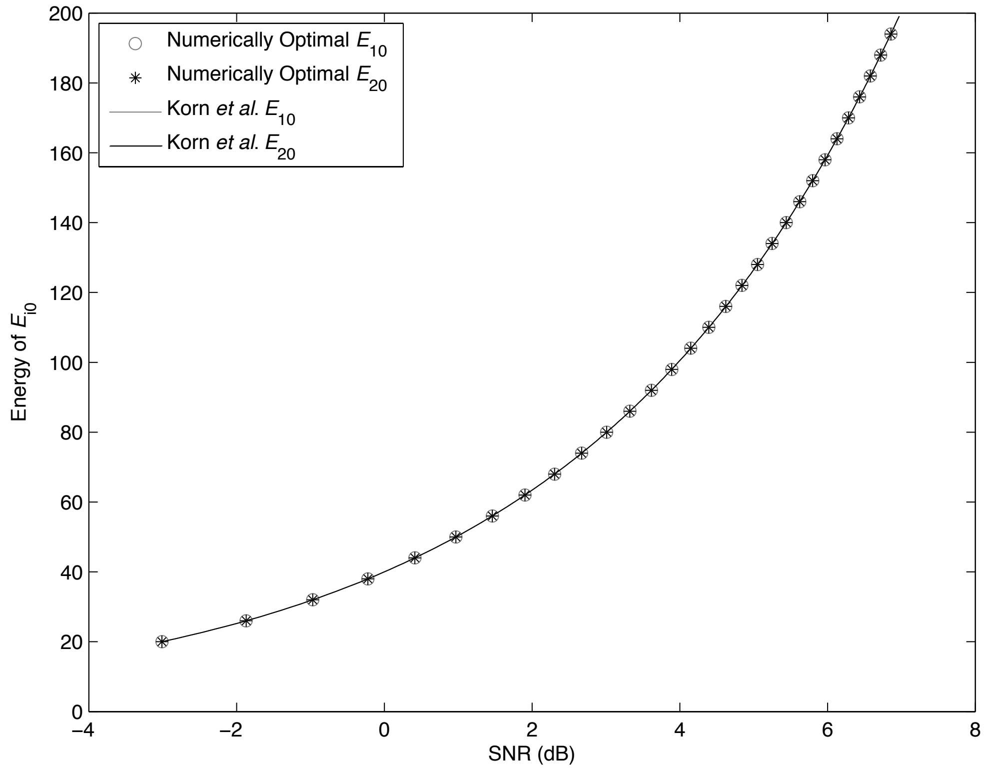

Figure 4.7: Numerical optimization vs. results in [1] when $\gamma = 1$ and $E_{10} = E_{20}$.

Combining this with (4.2) yields

$$\frac{\mu_{X_1}}{\sigma_{X_1}} = \frac{\lambda_{X_1}\sigma_1}{\sqrt{\left(\sqrt{\frac{E_1 - E_{10}p_1}{1-p_1}} - \sqrt{E_{10}}\gamma\right)^2}} + \frac{E_{10} - \frac{E_1 - E_{10}p_1}{1-p_1} + 2\left(\sqrt{\frac{E_1 - E_{10}p_1}{1-p_1}} - \sqrt{E_{10}}\gamma\right)\sqrt{E_{10}}\gamma}{2\sigma_1\sqrt{\left(\sqrt{\frac{E_1 - E_{10}p_1}{1-p_1}} - \sqrt{E_{10}}\gamma\right)^2}}.$$

The numerator of the second summation term is

$$E_{10} - \frac{E_1 - E_{10}p_1}{1 - p_1} + 2\left(\sqrt{\frac{E_1 - E_{10}p_1}{1 - p_1}} - \sqrt{E_{10}}\gamma\right)\sqrt{E_{10}}\gamma$$

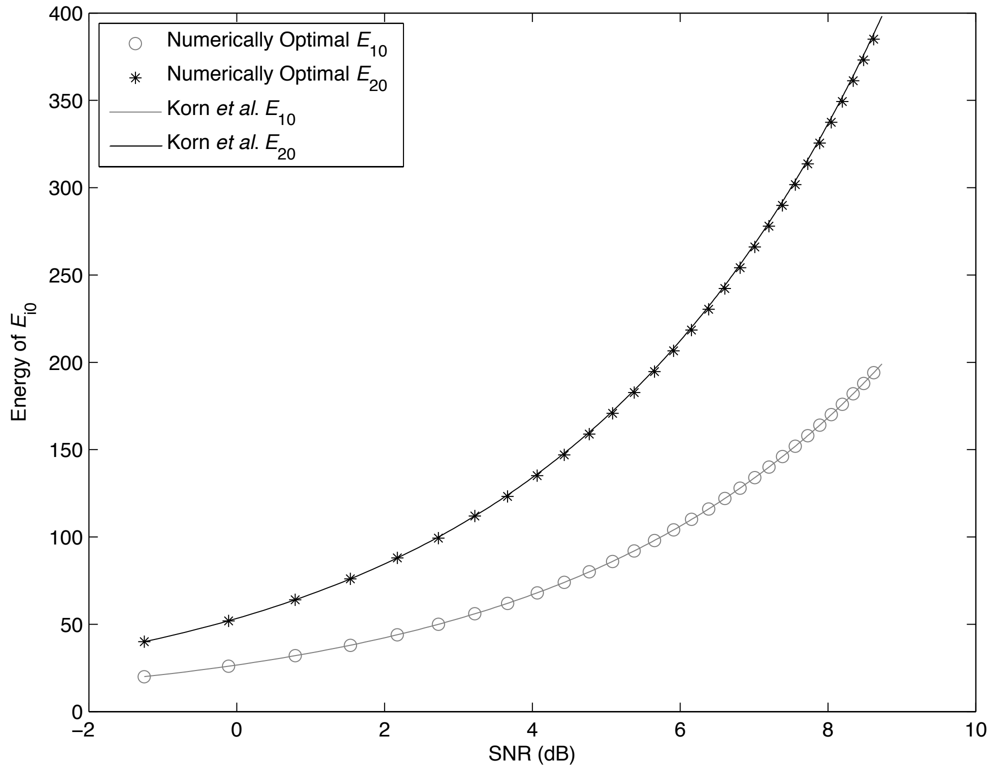

Figure 4.8: Numerical optimization vs. results in [1] when $\gamma = 1$ and $2E_{10} = E_{20}$.

$$= E_{10} - \frac{E_1 - E_{10}p_1}{1-p_1} + 2\sqrt{E_{10}}\sqrt{\frac{E_1 - E_{10}p_1}{1-p_1}}\gamma - 2E_{10}$$

$$= -\left(\sqrt{E_{10}}\gamma - \sqrt{\frac{E_1 - E_{10}p_1}{1-p_1}}\right)^2.$$

Letting

$$A_1 = \frac{\left(\sqrt{E_{10}}\gamma - \sqrt{\frac{E_1 - E_{10}p_1}{1-p_1}}\right)^2}{\sigma_1^2}$$

we can write

$$\frac{\mu_{X_1}}{\sigma_{X_1}} = \frac{\lambda_{X_1}}{\sqrt{A_1}} - \frac{\sqrt{A_1}}{2}.$$

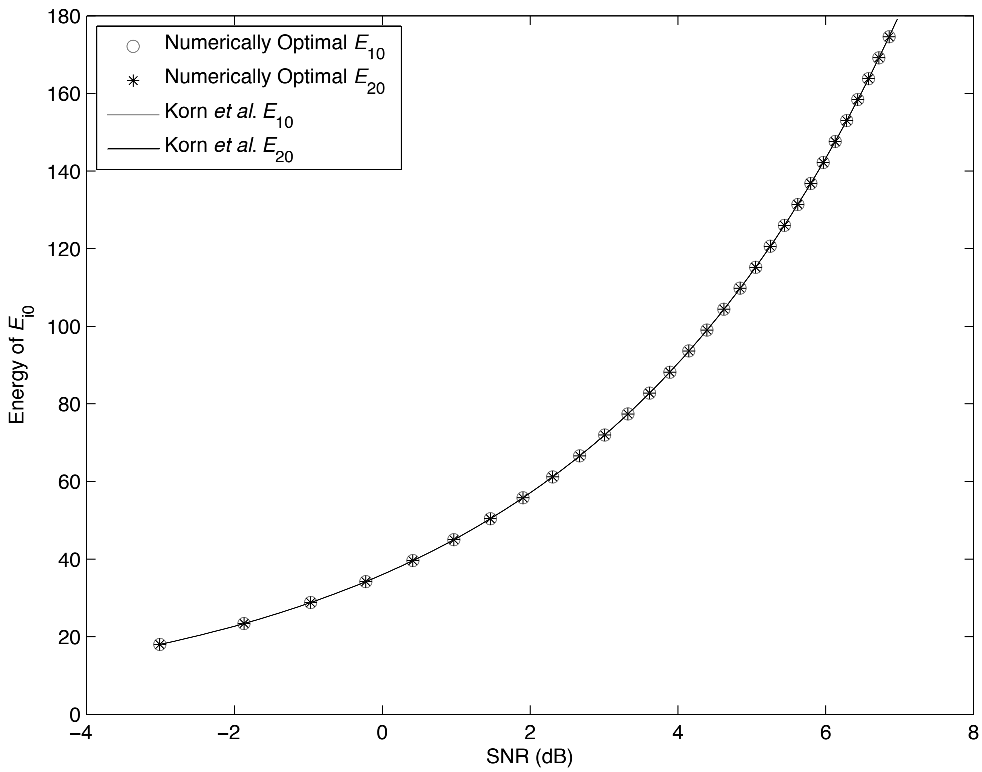

Figure 4.9: Numerical optimization vs. results in [1] when $\gamma = -1$ and $E_{10} = E_{20}$.

A similar derivation shows

$$\frac{\mu_{X_3}}{\sigma_{X_3}} = \frac{\lambda_{X_3}}{\sqrt{A_2}} - \frac{\sqrt{A_2}}{2}$$

where

$$A_2 = \frac{\left(\sqrt{E_{20}}\gamma - \sqrt{\frac{E_2 - E_{20}p_2}{1-p_2}}\right)^2}{\sigma_2^2} \text{ and } \lambda_{X_3} = \ln \frac{p_{U_1,U_2}(c(s_{10}), c(s_{21}))}{p_{U_1,U_2}(c(s_{10}), c(s_{20}))}.$$

Further, looking separately at the numerator and denominator of

$$\frac{\mu_{X_1} + \mu_{X_3} + \alpha}{\sqrt{\sigma_{X_1}^2 + \sigma_{X_3}^2}},$$

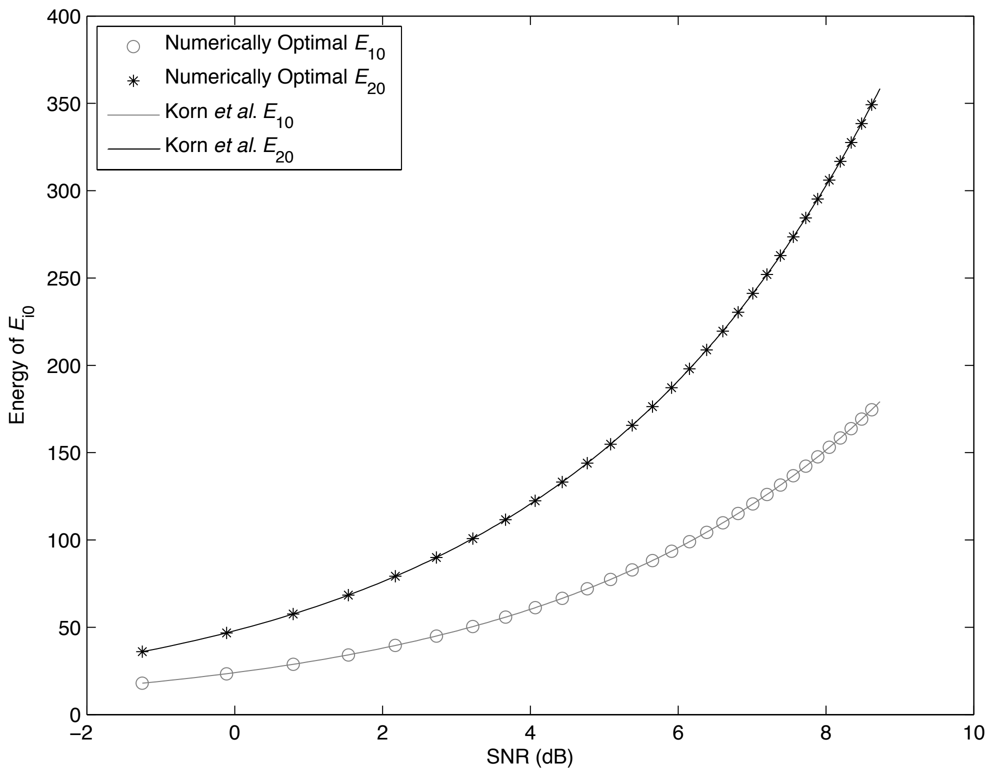

Figure 4.10: Numerical optimization vs. results in [1] when $\gamma = -1$ and $2E_{10} = E_{20}$.

we find

$$\begin{aligned}
\mu_{X_1} + \mu_{X_3} + \alpha &= \frac{E_{10} - E_{11}}{2\sigma_1^2} + \frac{s_{11} - s_{10}}{\sigma_1^2} s_{10} + \frac{E_{20} - E_{21}}{2\sigma_2^2} + \frac{s_{21} - s_{20}}{\sigma_2^2} s_{20} \\
&\quad + \lambda_{X_1} + \lambda_{X_3} + \alpha \\
&= \frac{E_{10} - \frac{E_1 - E_{10}p_1}{1-p_1} + 2\left(\sqrt{\frac{E_1 - E_{10}p_1}{1-p_1}} - \sqrt{E_{10}}\gamma\right)\sqrt{E_{10}}\gamma}{2\sigma_1^2} \\
&\quad + \frac{E_{20} - \frac{E_2 - E_{20}p_2}{1-p_2} + 2\left(\sqrt{\frac{E_2 - E_{20}p_2}{1-p_2}} - \sqrt{E_{20}}\gamma\right)\sqrt{E_{20}}\gamma}{2\sigma_2^2} \\
&\quad + \lambda_{X_1} + \lambda_{X_3} + \alpha \\
&= -\frac{A_1 + A_2}{2} + \lambda_{X_1} + \lambda_{X_3} + \alpha,
\end{aligned}$$

and

$$\begin{aligned}
\sqrt{\sigma_{X_1}^2+\sigma_{X_3}^2} &= \sqrt{\frac{(s_{11}-s_{10})^2}{\sigma_1^2}+\frac{(s_{21}-s_{20})^2}{\sigma_2^2}} \\
&= \sqrt{\frac{\left(\sqrt{E_{10}}\gamma-\sqrt{\frac{E_1-E_{10}p_1}{1-p_1}}\right)^2}{\sigma_1^2}+\frac{\left(\sqrt{E_{20}}\gamma-\sqrt{\frac{E_2-E_{20}p_2}{1-p_2}}\right)^2}{\sigma_2^2}} \\
&= \sqrt{A_1+A_2}.
\end{aligned}$$

Hence

$$\frac{\mu_{X_1}+\mu_{X_3}+\alpha}{\sqrt{\sigma_{X_1}^2+\sigma_{X_3}^2}} = \frac{\lambda_{X_1}+\lambda_{X_3}+\alpha}{\sqrt{A_1+A_2}} - \frac{\sqrt{A_1+A_2}}{2}.$$

Further, analogous arguments show that

$$\begin{aligned}
\frac{\mu_{Y_1}}{\sigma_{Y_1}} &= \frac{\lambda_{Y_1}}{\sqrt{A_1}} - \frac{\sqrt{A_1}}{2} \\
\frac{\mu_{Y_3}}{\sigma_{Y_3}} &= \frac{\lambda_{Y_3}}{\sqrt{A_2}} - \frac{\sqrt{A_2}}{2} \\
\frac{\mu_{Y_1}+\mu_{Y_3}+\alpha}{\sqrt{\sigma_{Y_1}^2+\sigma_{Y_3}^2}} &= \frac{\lambda_{Y_1}+\lambda_{Y_3}+\alpha}{\sqrt{A_1+A_2}} - \frac{\sqrt{A_1+A_2}}{2}
\end{aligned}$$

where

$$\lambda_{Y_1} = \ln[p_{U_1,U_2}(c(s_{10}),c(s_{21})))/(p_{U_1,U_2}(c(s_{11}),c(s_{21})))]$$

$$\lambda_{Y_3} = \ln[p_{U_1,U_2}(c(s_{11}),c(s_{20})))/(p_{U_1,U_2}(c(s_{11}),c(s_{21}))].$$

Note that, written in terms of A_1 or A_2, μ_{Z_1}/σ_{Z_1} and μ_{Z_3}/σ_{Z_3} are analogous to μ_{Y_1}/σ_{Y_1} and μ_{X_3}/σ_{Y_1}, respectively. Similarly, μ_{W_1}/σ_{W_1} and μ_{W_3}/σ_{W_3} are analogous to μ_{Y_1}/σ_{Y_1} and μ_{X_3}/σ_{X_3}, respectively. Lastly, the derivations of $(\mu_{Z_1}+\mu_{Z_3}-\alpha)/(\sqrt{\sigma_{Z_1}^2+\sigma_{Z_3}^2})$ and $(\mu_{W_1}+\mu_{W_3}-\alpha)/(\sqrt{\sigma_{W_1}^2+\sigma_{W_3}^2})$ are both analogous to $(\mu_{X_1}+$

$\mu_{X_3} + \alpha)/(\sqrt{\sigma_{X_1}^2 + \sigma_{X_3}^2})$. Thus, we can write (3.11) as

$$\begin{aligned}
P_{UB}(e) = &\left[3 - Q\left(\frac{\lambda_{X_1}}{\sqrt{A_1}} - \frac{\sqrt{A_1}}{2}\right) - Q\left(\frac{\lambda_{X_3}}{\sqrt{A_2}} - \frac{\sqrt{A_2}}{2}\right)\right.\\
&\left. - Q\left(\frac{\lambda_{X_1} + \lambda_{X_3} + \alpha}{\sqrt{A_1 + A_2}} - \frac{\sqrt{A_1 + A_2}}{2}\right)\right] P(c(s_{10}), c(s_{20}))\\
&+ \left[3 - Q\left(\frac{\lambda_{Y_1}}{\sqrt{A_1}} - \frac{\sqrt{A_1}}{2}\right) - Q\left(\frac{\lambda_{Y_3}}{\sqrt{A_2}} - \frac{\sqrt{A_1}}{2}\right)\right.\\
&\left. - Q\left(\frac{\lambda_{Y_1} + \lambda_{Y_3} + \alpha}{\sqrt{A_1 + A_2}} - \frac{\sqrt{A_1 + A_2}}{2}\right)\right] P(c(s_{11}), c(s_{21}))\\
&+ \left[3 - Q\left(\frac{\lambda_{Z_1}}{\sqrt{A_1}} - \frac{\sqrt{A_1}}{2}\right) - Q\left(\frac{\lambda_{Z_3}}{\sqrt{A_2}} - \frac{\sqrt{A_1}}{2}\right)\right.\\
&\left. - Q\left(\frac{\lambda_{Z_1} + \lambda_{Z_3} - \alpha}{\sqrt{A_1 + A_2}} - \frac{\sqrt{A_1 + A_2}}{2}\right)\right] P(c(s_{10}), c(s_{21}))\\
&+ \left[3 - Q\left(\frac{\lambda_{W_1}}{\sqrt{A_1}} - \frac{\sqrt{A_1}}{2}\right) - Q\left(\frac{\lambda_{W_3}}{\sqrt{A_2}} - \frac{\sqrt{A_1}}{2}\right)\right.\\
&\left. - Q\left(\frac{\lambda_{W_1} + \lambda_{W_3} - \alpha}{\sqrt{A_1 + A_2}} - \frac{\sqrt{A_1 + A_2}}{2}\right)\right] P(c(s_{11}), c(s_{20})) \qquad (4.3)
\end{aligned}$$

where

$$\lambda_{Z_1} = \ln[(p_{U_1,U_2}(c(s_{11}), c(s_{21})))/(p_{U_1,U_2}(c(s_{10}), c(s_{21})))]$$

$$\lambda_{Z_3} = \ln[(p_{U_1,U_2}(c(s_{10}), c(s_{20})))/(p_{U_1,U_2}(c(s_{10}), c(s_{21})))]$$

$$\lambda_{W_1} = \ln[(p_{U_1,U_2}(c(s_{10}), c(s_{20})))/(p_{U_1,U_2}(c(s_{11}), c(s_{20})))]$$

$$\lambda_{W_3} = \ln[(p_{U_1,U_2}(c(s_{11}), c(s_{21})))/(p_{U_1,U_2}(c(s_{11}), c(s_{20})))]$$

When showing (4.3) vanishes as SNR increased, we also show (3.9) vanishes, since recalling $0 \leq P(e) \leq P_{UB}(e)$. Looking at the terms in (4.3), we have

$$\begin{aligned}
\lim_{\sigma_1,\sigma_2 \to 0} &\left[3 - Q\left(\frac{\lambda_{V_1}}{\sqrt{A_1}} - \frac{\sqrt{A_1}}{2}\right) - Q\left(\frac{\lambda_{XV3}}{\sqrt{A_2}} - \frac{\sqrt{A_2}}{2}\right)\right.\\
&\left. - Q\left(\frac{\lambda_{V_1} + \lambda_{V_3} \pm \alpha}{\sqrt{A_1 + A_2}} - \frac{\sqrt{A_1 + A_2}}{2}\right)\right] = 0.
\end{aligned}$$

since as $\sigma_1, \sigma_2 \to 0$, $A_1, A_2 \to \infty$, and as $A_1, A_2 \to \infty$, $(\lambda_{V_1}/\sqrt{A_1}) - (\sqrt{A_1}/2) \to -\infty$, $(\lambda_{V_3}/\sqrt{A_2}) - (\sqrt{A_2}/2) \to -\infty$, and $(\mu_{V_1} + \mu_{V_3} \pm \alpha)/(\sqrt{\sigma_{V_1}^2 + \sigma_{V_3}^2}) - (\sqrt{\sigma_{V_1}^2 + \sigma_{V_3}^2})/2 \to -\infty$ for $V = X, YZ, W$. Lastly, note that $\lim_{x \to -\infty} Q(x) = 1$. Thus,

$$\lim_{\sigma_1, \sigma_2 \to 0} P(e) = \lim_{\sigma_1, \sigma_2 \to 0} P_{UB}(e) = 0.$$

4.3.2 Analytical Optimization of the Union Error Bound

Now, to minimize (3.11) we must maximize A_1 and A_2 with respect to E_{10} and E_{20}, respectively, by the same reasoning used to conclude that $\lim_{\sigma_1, \sigma_2 \to 0} P_{UB}(e) = 0$. We have

$$\begin{aligned}
\frac{\partial A_1}{\partial E_{10}} &= \frac{2A_1}{\sigma_1^2} \left(\frac{\gamma}{\sqrt{E_{10}}} - \frac{p_1}{(1-p_1)\sqrt{\frac{E_1 - p_1 E_{10}}{1-p_1}}} \right) \\
\frac{\partial^2 A_1}{\partial E_{10}^2} &= \frac{2}{\sigma_1^2} \frac{\gamma E_1^2 \sqrt{\frac{E_1 - p_1 E_{10}}{1-p_1}}}{2E_{10}^{3/2}(E_1 - p_1 E_{10})^2}.
\end{aligned}$$

Thus, for $\gamma = 1$, A_1 is a convex function with respect to E_{10}. As such the maximum will occur on a boundary point (recall that $E_{10} \in [0, E_1/p_1]$). Evaluating A_1 at the boundary points shows the maximum occurs at E_1/p_1. When $\gamma = -1$, A_1 is a concave function in E_{10}; thus, solving

$$\frac{\partial A_1}{\partial E_{10}} = \frac{A_1}{\sigma_1^2} \left(\frac{\gamma}{\sqrt{E_{10}}} - \frac{p_1}{(1-p_1)\sqrt{\frac{E_1 - p_1 E_{10}}{1-p_1}}} \right) = 0$$

shows the maximum occurs when

$$E_{10} = \frac{E_1(1 - p1)}{p_1}.$$

Hence, the results for E_{10} when $\gamma = 1$ and $\gamma = -1$ exactly coincide with (2.5) and (2.6), respectively. A similar analysis of A_2 yields the same results for E_{20}. Thus, analytic optimization of the union bound gives energy values which coincide with [1].

4.4 Performance Comparison

Since the optimal energies for our system coincide with that of [1]—the single-user case—it is interesting to examine if there exists a performance increase when using the optimal scheme from this report. To explore this question we consider three other modulation schemes. Recall from Chapter 3 that to fully describe the source we need $P(U_1 = 0) = p_1$, $P(U_2 = 0) = p_2$ and one of ρ or $p_{11} = P(U_1 = 1, U_2 = 1)$. The three schemes make different assumptions about the source statistics, although all schemes use the same source data; see Table 4.3 for detailed descriptions of the schemes. All schemes employ joint MAP detection at the demodulator, although for Schemes 1 and 2 this joint detection translates into parallel (single-user) detection.

It is important to note that Scheme 2 is two independent systems implementing the signalling schemes of [1] (here independence implies a correlation coefficient of zero). Further, note that Scheme 4 represents our system studied in Chapter 3 and Sections 4.1-4.3. Constellation points are determined using (2.5), (2.6), and (2.7). Lastly, modulation schemes prefaced with 'parallel' imply the use of two single-user detectors.

The values used in the simulations are: $\sigma_1 = \sigma_2 = 2$ and $E_1 \in [2, 20]$. In Figures 4.13 and 4.16, $E_2 = 2$ for all trials. Further, $p_1 = p_2 = 0.1$ and $\rho = 0.9$ unless otherwise specified by Table 4.3. Lastly, 4×10^6 source data pairs are transmitted for each curve.

Using the optimal energy allocation derived in the previous section, we consider the following simulation setup: for $\gamma = 1$, Figures 4.11 and 4.12 use $E_1 = E_2$ and

$2E_1 = E_2$, respectively. Further, in Figure 4.13, E_2 is a constant; in this case we observe the behaviour of the schemes when $E_1 \approx E_2$ at low SNR and $E_1 \gg E_2$ at high SNR. Similarly, for $\gamma = -1$, Figures 4.14, 4.15, and 4.16 use $E_1 = E_2$, $2E_1 = E_2$, and E_2 held constant, respectively.

From the figures in this section, the use of the optimal energy allocation used in Schemes 2 and 4 improves performance so long as $E_1 \not\gg E_2$ (see Figures 4.11-4.12 and 4.14-4.15). Further, in all scenarios Scheme 4 outperforms Schemes 1-3, since this scheme implements optimal energies and has knowledge of the source statistics in full. The possible gains, in terms of dB, using Scheme 4 over Schemes 1-3 are seen in Table 4.5.

In Figures 4.13 and 4.16 there is a SNR value in which Scheme 3 begins to perform better than Scheme 2. Recall, in these plots E_2 is constant. For arguments sake let us assume the source pair $(1, 1)$ is transmitted (since it is the most often transmitted signal at 89.1 percent) and Transmitter 1 communicates without error. Also take $\gamma = 1$. When SNR = 6 dB, then $E_1 = 46$ dB, the MAP detection for Scheme 2 fails when $N_2 > 2.11\sigma_2$, while MAP detection for Scheme 3 does not. However, when SNR = 1 dB, then $E_2 = 6$ dB. In this case, when $N_2 > 2.0\sigma_2$ MAP detection for Scheme 3 fails, whereas for MAP detection is correct of Scheme 2. Thus, low and high SNR's influence the MAP metrics of Scheme 2 and 3 differently, and the performance of these schemes changes accordingly.

		Scheme 1	Scheme 2	Scheme 3	Scheme 4
	Known Source Statistics	None	p_1 and p_2	ρ	p_1, p_2, and ρ
	Assumptions of Unknown Statistics	$p_1 = p_2 = 0.5$ and $\rho = 0$	$\rho = 0$	$p_1 = p_2 = 0.5$	None
$\gamma = 1$	Constellation Points	$s_{i0} = 2E_i$ $s_{i1} = 0$	$s_{i0} = E_i/p_i$ $s_{i1} = 0$	$s_{i0} = 2E_i$ $s_{i1} = 0$	$s_{i0} = E_i/p_i$ $s_{i1} = 0$
	Modulation Scheme	Parallel OOK	Parallel OOK	Joint OOK	Joint OOK
$\gamma = -1$	Constellation Points	$s_{i0} = -E_i$ $s_{i1} = E_i$	$s_{i0} = -\frac{E_i(1-p_i)}{p_i}$ $s_{i1} = \frac{E_i p_i}{(1-p_i)}$	$s_{i0} = -E_i$ $s_{i1} = E_i$	$s_{i0} = -\frac{E_i(1-p_i)}{p_i}$ $s_{i1} = \frac{E_i p_i}{(1-p_i)}$
	Modulation Scheme	Parallel Antipodal Signalling	Parallel BPAM	Joint Antipodal Signalling	Joint BPAM

Table 4.3: Description of the modulation schemes used for a performance comparison. All schemes use the same source, but different assumptions are made about the source statistics in each scheme.

	Gain from using Scheme 4 over:	Scheme 1	Scheme 2	Scheme 3
$\gamma = 1$	$E_1 = E_2$	> 9.87 dB	≈ 0.73 dB	> 9.87 dB
	$2E_1 = E_2$	> 9.87 dB	≈ 0.73 dB	≈ 7.83 dB
	$E_2 =$ constant	> 10.7 dB	> 10.7 dB	≈ 8.43 dB
$\gamma = -1$	$E_1 = E_2$	> 8.25 dB	≈ 0.73 dB	≈ 4.95 dB
	$2E_1 = E_2$	≈ 7.83 dB	≈ 0.73 dB	≈ 5.88 dB
	$E_2 =$ constant	> 10.7 dB	> 10.7 dB	≈ 7.17 dB

Table 4.4: Summary of gains possible when using our system (Scheme 4) over Schemes 1-3. Any value marked with a '>' represents the gains are greater the range of tested SNR values.

4.5 Optimization when $\gamma_1 = -\gamma_2$

First we note that as seen in Chapter 3 without loss of generality we let $\gamma_1 = 1$ and $\gamma_2 = -1$. Then when performing numerical analysis with the same values seen in Section 4.2, we find that the optimal values coincide with [1]; consult Table 4.6 for a comparison of the optimal energy allocation when numerically determined versus values from [1].

Further, we note that A_1 and A_2 can be written as follows

$$A_1 = \frac{\left(\sqrt{E_{10}}\gamma_1 - \sqrt{\frac{E_1 - E_{10}p_1}{1-p_1}}\right)^2}{\sigma_1^2}$$
$$A_2 = \frac{\left(\sqrt{E_{20}}\gamma_2 - \sqrt{\frac{E_2 - E_{20}p_2}{1-p_2}}\right)^2}{\sigma_2^2}.$$

Recall that $P_{UB}(e)$ is minimized when A_1 and A_2 are maximized. Further, since A_1 depends on E_1 and E_{10} only and A_2 depends on E_2 and E_{20} only, we can optimize these independently of one another. Thus, we have that (2.5) maximizes A_1 and (2.6) maximizes A_2. Thus, analytically and numerically the optimal energies when $\gamma_1 = 1$ and $\gamma_2 = -1$ coincide with [1].

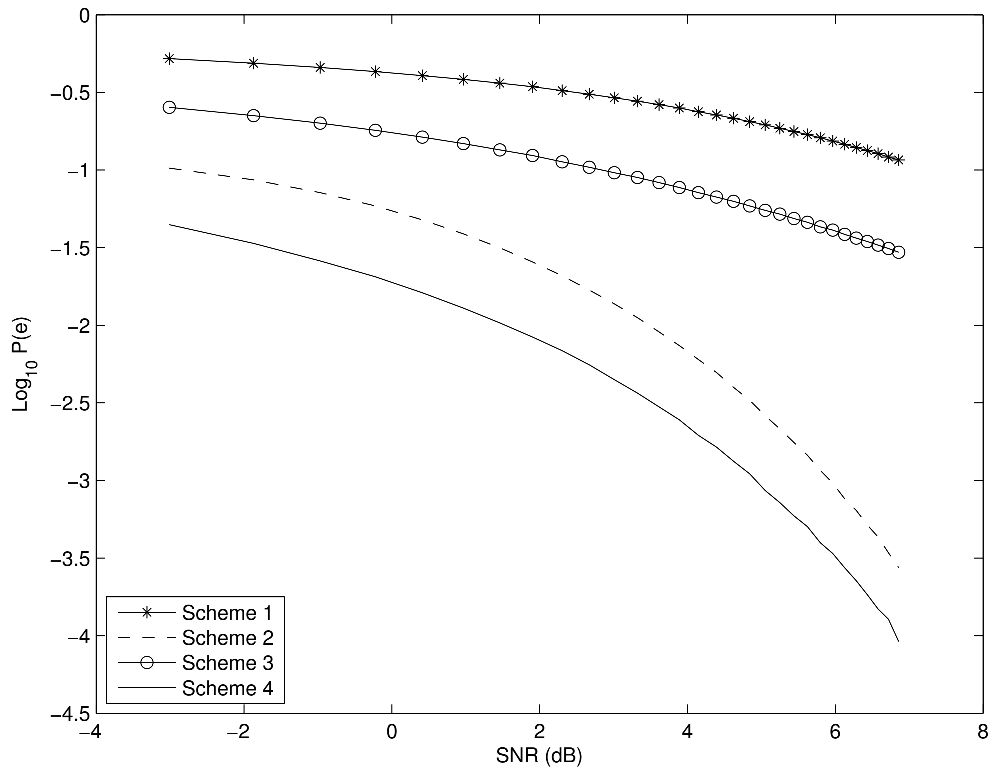

Figure 4.11: Comparison of schemes when $\gamma = 1$ and $E_1 = E_2$.

	Gain from using Scheme 4 over:	Scheme 1	Scheme 2	Scheme 3
	$E_1 = E_2$	> 9.87 dB	≈ 0.73 dB	> 9.87 dB
$\gamma = 1$	$2E_1 = E_2$	> 9.87 dB	≈ 0.73 dB	≈ 7.83 dB
	$E_2 =$ constant	> 10.7 dB	> 10.7 dB	≈ 8.43 dB
	$E_1 = E_2$	> 8.25 dB	≈ 0.73 dB	≈ 4.95 dB
$\gamma = -1$	$2E_1 = E_2$	≈ 7.83 dB	≈ 0.73 dB	≈ 5.88 dB
	$E_2 =$ constant	> 10.7 dB	> 10.7 dB	≈ 7.17 dB

Table 4.5: Summary of gains possible when using our system (Scheme 4) over Schemes 1-3. Any value marked with a '$>$' represents the gains are greater the range of tested SNR values.

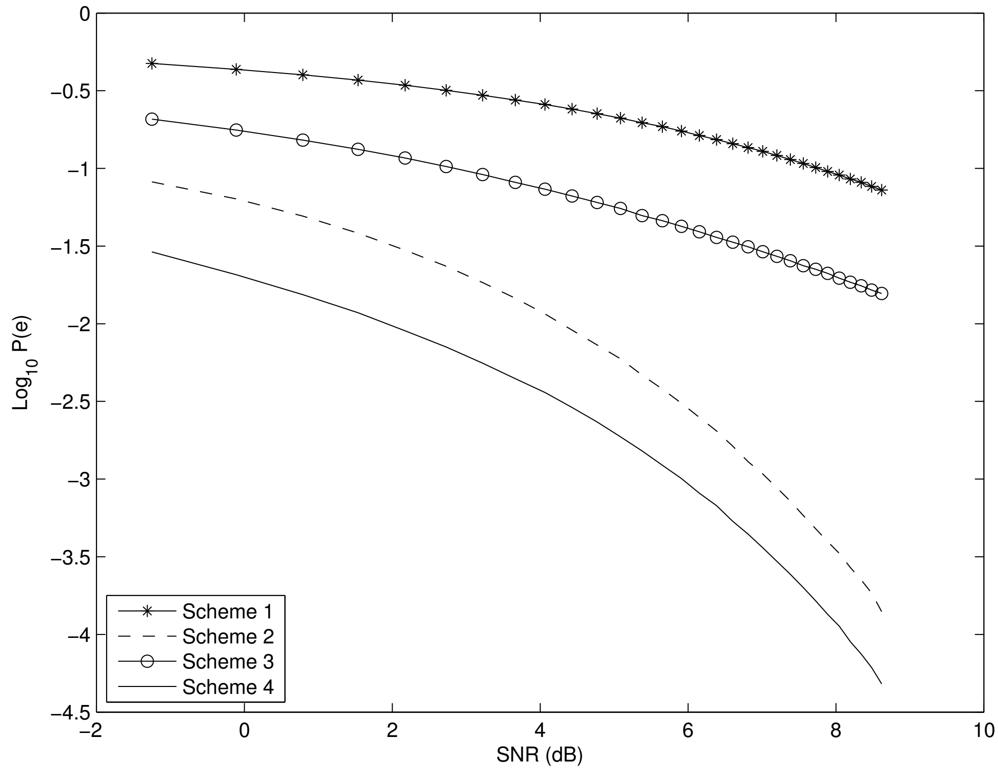

Figure 4.12: Comparison of schemes when $\gamma = 1$ and $2E_1 = E_2$.

We perform a similar performance comparison for the four schemes described in the previous section (using the same simulation values); in this case Transmitter 1 implements OOK, and Transmitter 2 implements BPAM. Here there are five possible scenarios since $\gamma_1 = 1$ and $\gamma_2 = -1$. These scenarios are $E_1 = E_2$, $2E_1 = E_2$, $E_1 = 2E_2$, E_1 is constant and E_2 is a constant. However, we only present the best performing scheme of $E_1 = E_2$ and $2E_1 = E_2$. We do the same for the case where E_1 is constant and where E_2 is a constant, respectively. Figures 4.17, 4.18, and 4.19 correspond to $E_1 = E_2$, $2E_1 = E_2$ and E_1 constant, respectively, where we note that the performance curves are similar to those seen in the previous section. In particular when E_1 is constant we get the crossover in performance between Schemes 2 and 3. The explanation of this crossover in the previous section holds here. Lastly,

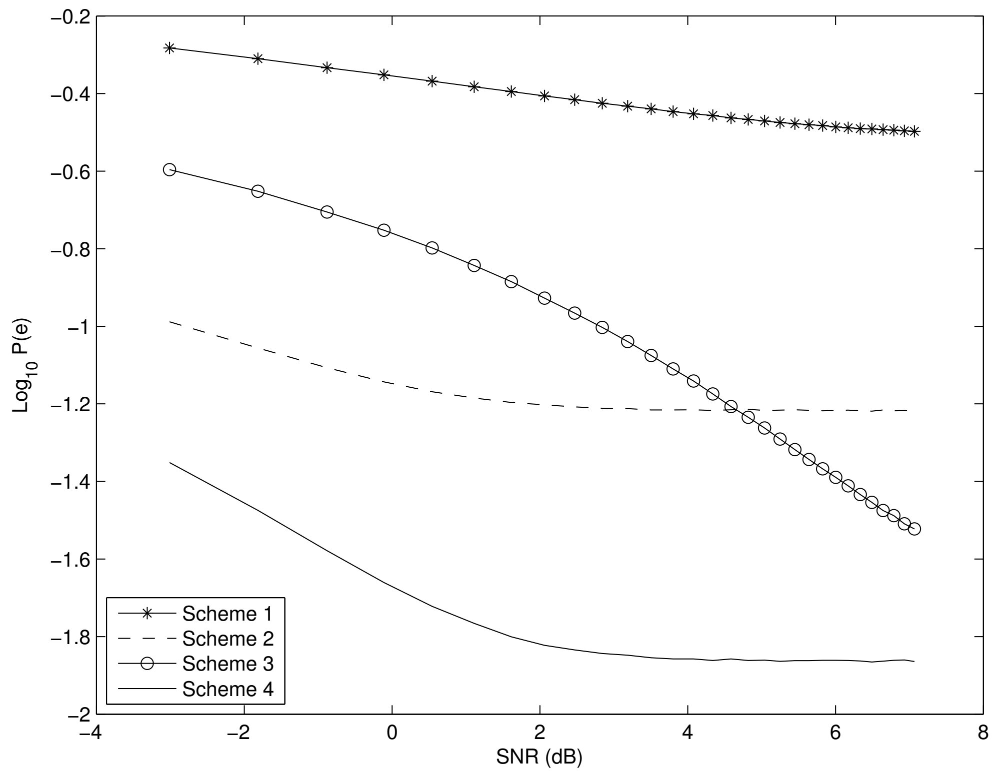

Figure 4.13: Comparison of schemes when $\gamma = 1$ and E_2 is a constant.

	Numerically optimal E_{10}	E_{10} from [1]	Numerically optimal E_{20}	E_{20} from [1]
$E_1 = E_2$	100	90	100	90
$2E_1 = E_2$	100	180	100	180
$E_1 = 2E_2$	200	90	200	90

Table 4.6: Comparison of our numerical optimization results and [1] for $\gamma_1 = 1$ and $\gamma = -1$.

note for Figures 4.17, 4.18, and 4.19 our scheme (Scheme 4) performs best, with at least 0.73 dB, 0.73 dB, and 6.85 dB increase in performance over the other schemes, respectively.

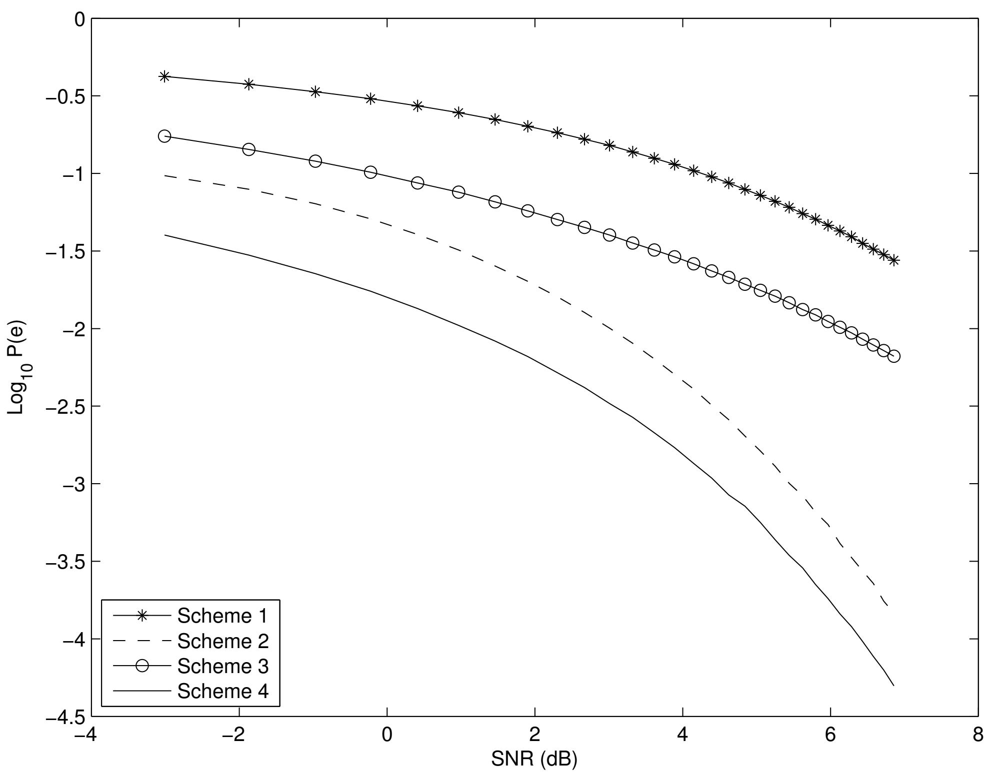

Figure 4.14: Comparison of schemes when $\gamma = -1$ and $E_1 = E_2$.

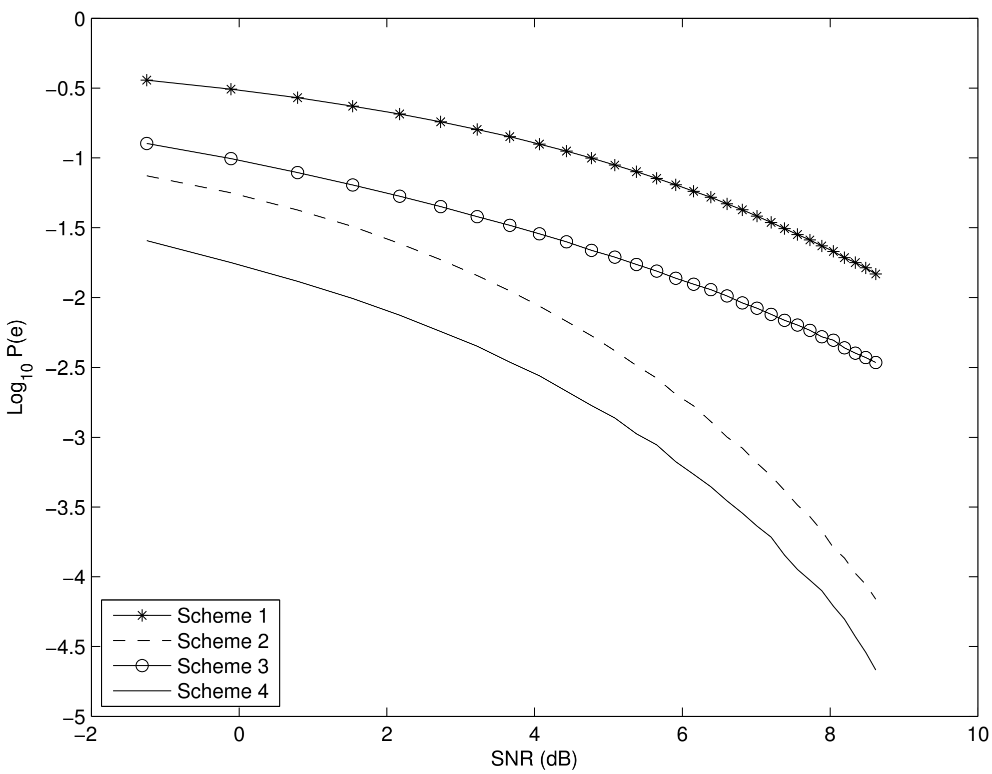

Figure 4.15: Comparison of schemes when $\gamma = -1$ and $2E_1 = E_2$.

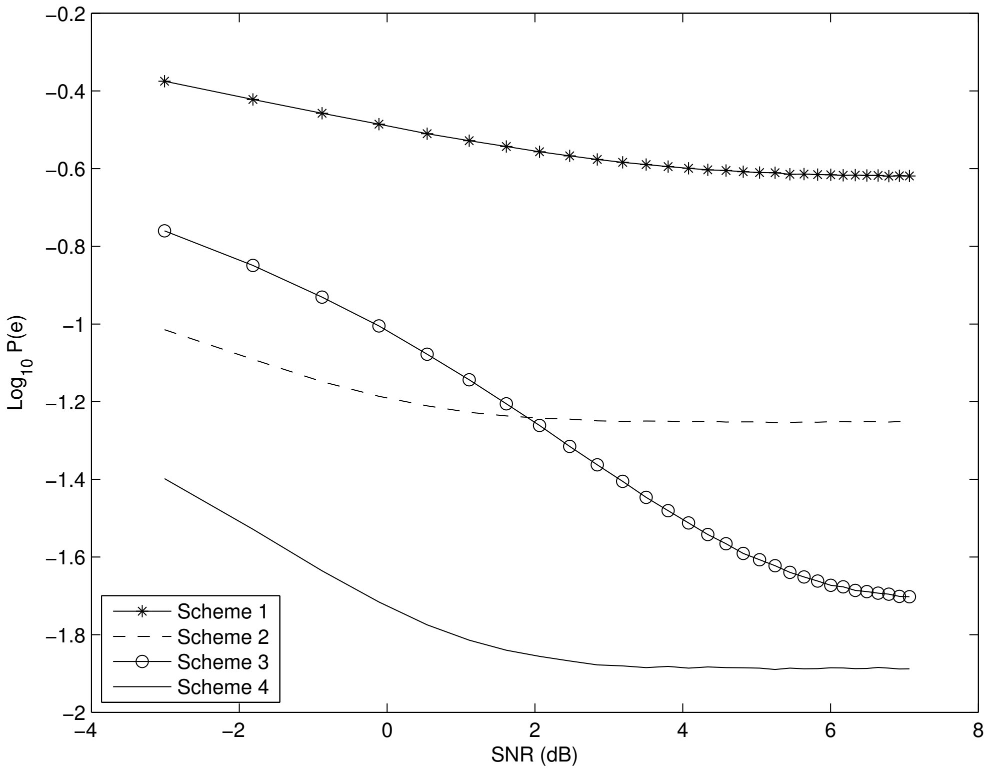

Figure 4.16: Comparison of schemes when $\gamma = -1$ and E_2 is a constant.

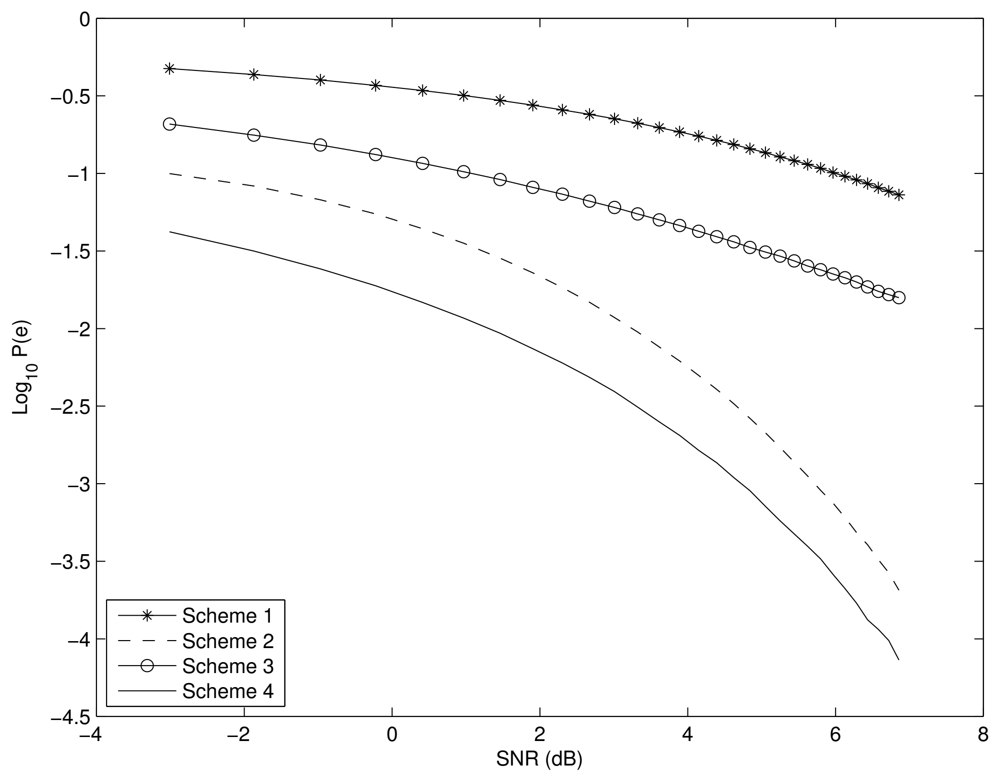

Figure 4.17: Comparison of schemes when $-\gamma_2 = \gamma_1 = 1$ and $E_1 = E_2$.

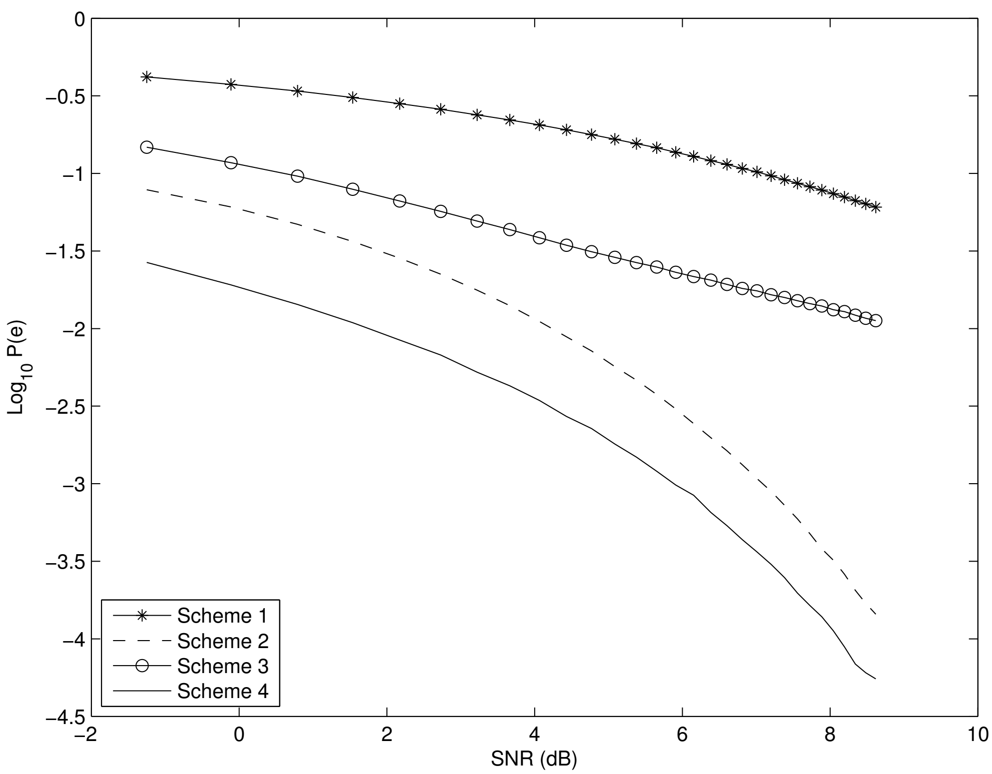

Figure 4.18: Comparison of schemes when $-\gamma_2 = \gamma_1 = 1$ and $2E_1 = E_2$.

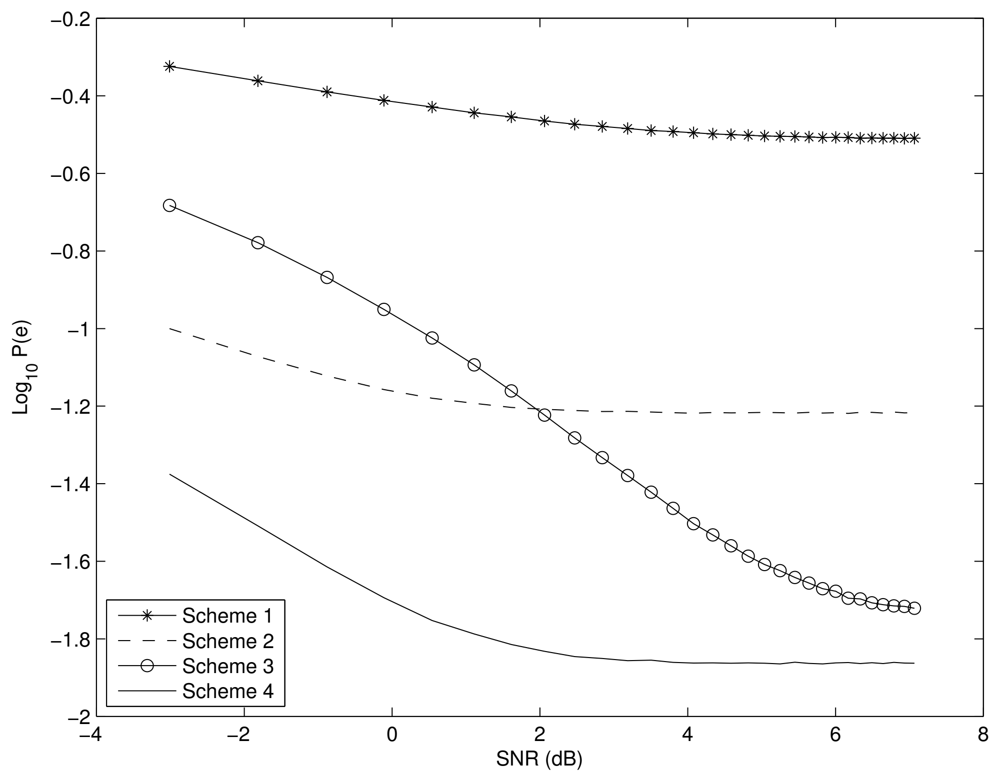

Figure 4.19: Comparison of schemes when $-\gamma_2 = \gamma_1 = 1$ and E_1 is constant.

Chapter 5

Conclusion and Future Work

5.1 Conclusion

In this report we have shown that for the orthogonal multiple access Gaussian channel, with nonequiprobable correlated sources, the optimal transmission energies coincide with those seen in [1] for the single-user case. As shown in Chapter 3, three parameters are needed to describe the source. The optimized OMAGC is compared to three schemes which vary how many the three source parameters are known. A gain of at least 0.73 dB is achieved when $E_1 = E_2$ or $2E_1 = E_2$, where E_1 and E_2 are the given average energies of Transmitters 1 and 2, respectfully. When $E_1 \gg E_2$ a gain of at least 7 dB is seen. Further we have shown that our system, which knows all three parameters of the source, outperforms all those other schemes.

5.2 Future Work

A next step would to be consider arbitrary correlation between basis functions. In doing so, an interesting alteration could be made to the system model. Namely, one can replace the orthogonal channels with a 'additive Gaussian' channel, where the two transmitted signals are added to one another and then transmitted across the channel. In this case there is one noise term. To be specific, using notation from

Chapter 3, $\boldsymbol{r} = \boldsymbol{s}_1 + \boldsymbol{s}_2 + N$, where N is a $N(0, \sigma^2)$ random variable. As in this document, it would be interesting to see if the optimal energies coincide with [1].

Appendix A

Complementary Calculations

A.1 Sign Change In α

In Chapter 3, the terms denoted with Z, W cause a sign change in α. Since the two cases are analogous we consider the terms denoted by Z. Consider

$$\begin{aligned}
Z_1 &= \ln \frac{p_{U_1,U_2}(c(s_{11}), c(s_{21}))}{p_{U_1,U_2}(c(s_{10}), c(s_{21}))} + \frac{E_{10} - E_{11}}{2\sigma_1^2} + \frac{s_{11} - s_{10}}{\sigma_1^2} R_1 \\
Z_3 &= \ln \frac{p_{U_1,U_2}(c(s_{10}), c(s_{20}))}{p_{U_1,U_2}(c(s_{10}), c(s_{21}))} + \frac{E_{21} - E_{20}}{2\sigma_2^2} + \frac{s_{20} - s_{21}}{\sigma_2^2} R_2 \\
Z_2 &= \ln \frac{p_{U_1,U_2}(c(s_{11}), c(s_{20}))}{p_{U_1,U_2}(c(s_{10}), c(s_{21}))} + \frac{E_{10} - E_{11}}{2\sigma_1^2} + \frac{s_{11} - s_{10}}{\sigma_1^2} R_1 \\
&\quad + \frac{E_{21} - E_{20}}{2\sigma_2^2} + \frac{s_{20} - s_{21}}{\sigma_2^2} R_2.
\end{aligned}$$

Then,

$$\begin{aligned}
Z_2 &= \ln \frac{p_{U_1,U_2}(c(s_{11}), c(s_{20}))}{p_{U_1,U_2}(c(s_{10}), c(s_{21}))} + Z_1 - \ln \frac{p_{U_1,U_2}(c(s_{11}), c(s_{21}))}{p_{U_1,U_2}(c(s_{10}), c(s_{21}))} \\
&\quad + Z_3 - \ln \frac{p_{U_1,U_2}(c(s_{10}), c(s_{20}))}{p_{U_1,U_2}(c(s_{10}), c(s_{21}))} \\
&= Z_1 + Z_3 + \ln p_{U_1,U_2}(c(s_{11}), c(s_{20})) - \ln p_{U_1,U_2}(c(s_{10}), c(s_{21})) \\
&\qquad - \ln p_{U_1,U_2}(c(s_{11}), c(s_{21})) + \ln p_{U_1,U_2}(c(s_{10}), c(s_{21}))
\end{aligned}$$

$$
\begin{aligned}
&- \ln p_{U_1,U_2}(c(s_{10}), c(s_{20})) + \ln p_{U_1,U_2}(c(s_{10}), c(s_{21})) \\
&= Z_1 + Z_3 + \ln \frac{p_{U_1,U_2}(c(s_{10}), c(s_{21}))p_{U_1,U_2}(c(s_{11}), c(s_{20}))}{p_{U_1,U_2}(c(s_{10}), c(s_{20}))p_{U_1,U_2}(c(s_{11}), c(s_{21}))}.
\end{aligned}
$$

However, (3.7) gives

$$
\alpha = \ln \frac{p_{U_1,U_2}(c(s_{10}), c(s_{20}))p_{U_1,U_2}((c(s_{11}), c(s_{21}))}{p_{U_1,U_2}(c(s_{11}), c(s_{20}))p_{U_1,U_2}(c(s_{10}), c(s_{21}))};
$$

then

$$
\begin{aligned}
-\alpha &= -\ln \frac{p_{U_1,U_2}(c(s_{10}), c(s_{20}))p_{U_1,U_2}((c(s_{11}), c(s_{21}))}{p_{U_1,U_2}(c(s_{11}), c(s_{20}))p_{U_1,U_2}(c(s_{10}), c(s_{21}))} \\
&= \ln \left[\frac{p_{U_1,U_2}(c(s_{10}), c(s_{20}))p_{U_1,U_2}((c(s_{11}), c(s_{21}))}{p_{U_1,U_2}(c(s_{11}), c(s_{20}))p_{U_1,U_2}(c(s_{10}), c(s_{21}))} \right]^{-1} \\
&= \ln \frac{p_{U_1,U_2}(c(s_{10}), c(s_{21}))p_{U_1,U_2}(c(s_{11}), c(s_{20}))}{p_{U_1,U_2}(c(s_{10}), c(s_{20}))p_{U_1,U_2}(c(s_{11}), c(s_{21}))}.
\end{aligned}
$$

Thus,

$$
Z_2 = Z_1 + Z_3 - \alpha
$$

and by the same reasoning

$$
W_2 = W_1 + W_3 - \alpha.
$$

Bibliography

[1] I. Korn, J. Fonseka and S. Xing, "Optimal Binary Communication With Nonequal Probabilities," IEEE Transactions on Communications, vol. 51, pp. 1435-1438, Sept. 2003.

[2] J.G. Proakis and Masoud Salehi, *Communication Systems Engineering, Second Edition*, Upper Saddle River: Pearson, 2002.

[3] F. Alajaji, N. Phamdo, and T. Fuja, "Channel Codes That Exploit the Residual Redundancy in CELP-Encoded Speech," IEEE Transactions on Speech and Audio Processing , Vol. 4, No. 5, pp. 325-336, September 1996.

[4] H. Kuai, F. Alajaji and G. Takahara,"Tight Error Bounds for Nonuniform Signalling over AWGN Channels," IEEE Transactions on Information Theory, Vol. 46, No. 7, November 2000.

[5] P. Z. Peebles, *Digital Communication Systems*. Englewood Cliffs, NJ: Prentice-Hall, 1987.

[6] J. Kron, F. Alajaji and M. Skoglund, "Low-Delay Joint Source-Channel Mappings for the Gaussian MAC", IEEE Communications Letters, Vol. 18, No. 2, February 2014.